OPTIMIZATION AND MODELING OF MULTIMODAL ACTIVE DEBRIS REMOVAL USING A TIME-EXPANDED NETWORK

A Thesis
Presented to
The Academic Faculty

By

Julia Tepper

In Partial Fulfillment
of the Requirements for the Degree
Master of Science in the
Daniel Guggenheim School of Aerospace Engineering

Georgia Institute of Technology

May 2023

OPTIMIZATION AND MODELING OF MULTIMODAL ACTIVE DEBRIS REMOVAL USING A TIME-EXPANDED NETWORK

Thesis committee:

Dr. Koki Ho, Advisor
Daniel Guggenheim School of Aerospace Engineering
Georgia Institute of Technology

Dr. Brian C. Gunter
Daniel Guggenheim School of Aerospace Engineering
Georgia Institute of Technology

Dr. E. Glenn Lightsey
Daniel Guggenheim School of Aerospace Engineering
Georgia Institute of Technology

Date approved: April 26, 2023

ACKNOWLEDGMENTS

I would like to extend my sincere gratitude to my advisor, Prof. Koki Ho, for his continuous support throughout my masters research. His guidance and immense knowledge were incredibly valuable, and he has helped me to become a better student, researcher, and engineer.

I would additionally like to acknowledge my other committee members, Prof. Glenn Lightsey and Prof. Brian Gunter, for their support both in and out of the classroom, graciously offering their insight and guidance to this thesis.

I would also like to thank the members of the Space Systems Optimization Group for their morale and encouragement. I am lucky to have been able to work alongside some of the brightest minds at Georgia Tech.

I would also like to thank Youssof Fassi, Tristan Sarton Du Jonchay, and Yuri Shimane, who contributed to the work presented here. Additionally, this material is based upon work that was supported by the Georgia Tech Research Institute.

Also, special thanks to my family, for their endless love and support.

TABLE OF CONTENTS

LIST OF TABLES

LIST OF FIGURES

LIST OF NOMENCLATURE

Δt A period of time in the time-expanded network

Δt_h Length of the debris removal portion of Δt

Δt_t Length of the travel portion of Δt

ΔV_{ijtq} ΔV for the ADR Vehicle to fly from i to j in time q starting at time t

$\mathcal{N}$ The set of all debris nodes and start node

$\mathcal{N}_d$ The set of all debris nodes in $\mathcal{N}$

$\mathcal{N}_p$ The set of all start nodes in $\mathcal{N}$

$\mathcal{N}_{dl}$ The set of all large debris nodes in $\mathcal{N}_d$

$\mathcal{N}_{ds}$ The set of all small debris nodes in $\mathcal{N}_d$

$\mathcal{Q}$ The set of time of flight maneuvers

$\mathcal{T}$ The set of time steps

$\mathcal{T}_h$ The set of time steps followed by Δt_h

$\mathcal{T}_t$ The set of time steps followed by Δt_t

ψ The minimum desired number of debris for removal

A_{it} Small debris removal device variable over holdover arcs

B_{it} Large debris removal device variable over holdover arcs

c_{ad} The small debris removal device capacity of the ADR Vehicle

c_{be} The large debris removal device capacity of the ADR Vehicle

c_{zw} The propellant capacity of the ADR Vehicle

d Number of debris removal devices deployed at debris node i

D_{ijtq} Small debris removal device variable over transportation arcs

E_{ijtq} Large debris removal device variable over transportation arcs

g_0 Gravitational acceleration

H_{it} Service variable over holdover arcs

i, j The index set for $\mathcal{N}$

I_{sp} Specific impulse

m_{ADRV} Structural mass of the ADR Vehicle

$m_{\text{DRD,Large}}$ Mass of one large debris removal device

$m_{\text{DRD,Small}}$ Mass of one small debris removal device

$m_{p,\text{max}}$ Maximum propellant value to search in the binary search algorithm

$m_{p,\text{min}}$ Minimum propellant value to search in the binary search algorithm

q The index set for $\mathcal{Q}$

r_{ijtq} Propellant consumption factor

T Maximum length of the ADR mission

t The index set for $\mathcal{T}$

U_{ijtq} ADR Vehicle variable over transportation arcs

$W^{\pm}_{ijtq}$ Propellant variable over transportation arcs

w_{it} The reward for removing debris i at time t

X_{it} ADR Vehicle variable over holdover arcs

$Z^{\pm}_{it}$ Propellant variable over holdover arcs

SUMMARY

This thesis develops a framework to optimize the concept of operations of an active debris removal (ADR) mission targeting variable sizes and types of space debris. Given the challenging and costly nature of active debris removal, it is desirable to minimize the required ΔV and propellant of the mission while maximizing the reward from debris removed to determine the most optimal sequence and subset of debris to remove. Potentially damaging debris ranges in size and mass from very small microdebris to much larger debris. Removal of these different types of debris involves different mission requirements. This thesis investigates the feasibility and optimality of removing both types of debris in one mission to maximize potential reward.

The optimization framework to design a mission to combine removal of both of these types of debris consists of a trajectory model to simulate orbital maneuvers throughout the mission as well as a mathematical formulation constructed as a Mixed-Integer Linear Problem. Orbital maneuvers between debris pairs are modeled as high-thrust two-impulse maneuvers, and the minimum ΔV for each maneuver at each time step between each pair of debris is determined. Next, the dynamic traveling salesperson problem is formulated as a Mixed-Integer Linear Problem. Solving a traveling salesperson problem with variable costs due to the dynamic nature of space debris is simplified by the use of a time-expanded network. The Mixed-Integer Linear Problem is then iteratively solved to optimize the mission for dual objectives. Using this formulation, an optimal mission scenario with a subset of targeted debris can efficiently and accurately be computed from a large set of potential debris for removal. Several case studies demonstrate the efficacy of this approach, examining missions to stabilize the debris environment by removing at least five pieces of debris over one year.

CHAPTER 1

INTRODUCTION

Space debris in low-Earth orbit is a problem that threatens current and future space missions. Satellites in low-Earth orbit are critical infrastructure for military, scientific, and commercial services. As rocket launches and satellites in LEO become increasingly accessible, the population in orbit will continue to increase. There are currently around 20,000 observable objects orbiting Earth. However, there are only about 2,200 operational satellites. Therefore about 18,000 tracked objects, or 90% of the total orbital population, are space debris [1].

The Kessler effect, first identified in 1978 by Kessler and Cour-Palais, is a hypothesized event where the number of space debris in orbit would grow at an uncontrollable and exponential rate until the future debris environment is dominated by accidental debris fragments [2]. In this scenario, the density of objects in low Earth orbit is high enough so that collisions between objects create a cascade in which each collision creates space debris, increasing the likelihood of further collisions. In 2009, Iridium 33 and Cosmos 2251 collided, creating an additional estimated 2,000 additional pieces of debris [3] and highlighting the potential dangers of the Kessler effect. To avoid this scenario, debris mitigation and removal strategies are necessary.

Debris mitigation strategies, such as limiting the number of new launches and imposing a necessary graveyard deorbit, are likely not enough to maintain a sustainable space environment for future missions. Even if no future launches occurred, collisions by existing satellites would increase the number of debris fragments faster than atmospheric drag would remove them [4]. It is imperative to investigate active debris removal (ADR) strategies to remove debris. Liou et al. found that it is only necessary to remove five large pieces of debris per year in addition to imposing mandatory deorbiting strategies for new launches to stabilize the orbital environment [5]. This low requirement suggests that ADR may be feasible to mitigate space debris in orbit. Since ADR is expensive and technically challenging, optimizing the debris removal strategy for its cost and reward of debris removal is imperative.

In 2023, NASA published a comprehensive cost-benefit analysis of orbital debris remediation [6]. This report presents a cost-benefit analysis considering various approaches to debris remediation and evaluating their potential costs versus their potential short-term and long-term benefits. Notably, the authors considered two distinct types of space debris: large, trackable debris consisting primarily of defunct rocket boosters and retired spacecraft and small debris ranging in size from 1-10 cm. Although large debris poses a more catastrophically destructive potential to active satellites and creates the potential to fragment into more pieces of debris, small debris poses risks since it is difficult to track and maneuver around in advance to avoid damage. The importance of addressing and removing both types of debris was stressed.

Potential removal methods were estimated, and an associated cost was presented for each removal method. Similarly, a monetary benefit for removing each piece of debris is estimated. The report concluded that addressing both small and large debris is most beneficial for maintaining the sustainability of the orbital environment. Assessing the feasibility and optimality of combining removal of both large and small debris in one ADR mission is desirable. For this reason, a multimodal approach to ADR is investigated in this thesis, attempting to target both small and large debris in one mission. The presented approach attempts to evaluate this hypothetical mission's feasibility and potential reward.

ADR is a complex problem involving many variables that requires thorough optimization. The debris environment constantly moves and orbits the Earth, creating a nonstatic network. Additionally, the trajectory of the ADR Vehicle can be evaluated as a dynamic traveling salesperson problem, with different costs associated with traveling from one debris to the next. There are variable travel and collection times associated with debris removals and orbital maneuvers. There are also potentially tens of thousands of debris in low-Earth orbit that can be considered for removal. All of these challenges increase the complexity of the optimization problem. This thesis presents a logistics formulation modeled as a Mixed-Integer Linear Problem (MILP) utilizing a time-expanded network, which discretizes both the removal times and the travel times for the ADR Vehicle between each debris. This MILP is iteratively solved to determine the minimum-cost mission that will maximize reward associated with debris removal.

In the current research on optimizing ADR missions, most approaches utilize a similar method. In these methods, time is treated as a variable in their optimization formulation so that time between orbital maneuvers is optimized along with the sequence of debris to remove. This approach results in long computational times and a limited number of pieces of debris that are able to be considered in the optimization. Additionally, these methods fail to utilize several key features of the ADR problem statement.

Several papers have devised methods for ADR mission optimization. In particular, Shen et al. [7] and Yu et al. [8] evaluated feasible mission designs by estimating transfer times and ΔV between all possible sequences, then optimizing the traveling salesperson problem using a bi-objective optimization. Berend and Olive [9] used a similar bi-objective optimization framework, minimizing the total mission duration as well as the debris sequence. Much of the surveyed literature used differing optimization strategies as well. Kanazaki et al. [10] evaluated optimal mission scenarios using a traveling salesperson problem optimized using an evolutionary algorithm, whereas Zhang et al. [11] evaluated the traveling salesperson problem using ant colony optimization. Similarly, Federici et al. [12] and Missel and Mortari [13] solved the traveling salesperson problem using simulated methods. Lastly, Federici et al. [14] solved the traveling salesperson problem using A*. In this optimal tree search algorithm, they optimized a cluster of as many as 21 pieces of debris. Lee, Lee, and Ahn [15] similarly attempt to solve the multitarget rendezvous problem by decomposing the problem into a two-phase framework. They first create a multi-layer elementary solution database to generate two-impulse and three-impulse optimal transfer solutions between two targets. Then, they formulate and solve the combinatorial optimization problem. Although each approach varied slightly in their methods to estimate and optimize orbital maneuvers and the methods used to optimize the traveling salesperson problem, they all set time as a variable, producing a more complex formulation.

Bang and Ahn [16] presented a two-phase framework for near-optimal multitarget Lambert rendezvous, examining an asteroid exploration case study using their framework. The framework consists of two phases: first, a series of single-target rendezvous problems for all departure-arrival object pairs are solved to generate elementary solutions. Second, a variant of the traveling salesperson problem is formulated using the elementary solutions and determining the final rendezvous sequence and trajectories. This approach differs from our presented approach in several ways. First, the first phase of their approach employs variable transfer times, considering the transfer time for the spacecraft to be a decision variable. The timeline changes based on the lowest-cost possible sequence and is not fixed. In Bang and Ahn's presented approach to multitarget rendezvous for ADR using multiple spacecraft [17], another two-phase framework is shown for effectively solving an ADR problem that utilizes multiple chaser spacecraft. Additionally, both long and short mission durations are considered. Two-impulse Lambert maneuvers and three-phase maneuvers using RAAN drift are employed for each mission duration, respectively. In determining the time that the maneuver takes, departure and arrival times are treated as design variables. Although this approach mimics the approach presented herein that not all debris considered is necessarily selected for removal, it differs primarily in terms of formulation and approach. In our framework, time is treated as a parameter rather than a variable. Additionally, our approach focuses on the optimization of just one removal spacecraft.

Time-expanded networks have successfully been used to solve other complex space logistics problems, such as the work done by Sarton du Jonchay et al. considering on-orbit servicing [18]. This thesis seeks to use a time-expanded network to simplify the complexities of the dynamic network. Using this formulation, an optimal mission scenario can efficiently and accurately be computed from a large set of potential debris for removal. Using a time-expanded network removes time from the list of decision variables considered, and standardizes it across all debris removals and maneuvers. This approach produces a method that can deliver results quickly and consider a large debris set. A time-expanded network is a natural solution to the ADR problem. Since a minimum of five pieces of debris per year need to be removed to stabilize the debris environment, it is beneficial to standardize the time variable to allow for five or more debris per year to be removed and allow the optimizer to select the subset of debris that produces the highest-reward mission to achieve this goal [19].

The methods introduced in this thesis can select the most optimal subset of space debris to remove from a much more extensive list of considered debris to maximize reward and minimize propellant cost. The optimization objectives are to determine the mission that will obtain the maximum possible reward from debris removal given the mission parameters while minimizing the ΔV and propellant required to obtain this reward. This method employs a multimodal approach to address all types of potentially damaging debris, considering the potential combination of small and large debris removals in a single mission. This method is also highly generalizable, as the ability to modify the number of time steps to change the number of debris removed as well as other mission parameters allows the optimizer to evaluate different scenarios with different numbers of removals.

Out of the large space debris population, it is essential to prioritize the most concerning and potentially damaging pieces of debris. McKnight et al. analyzed large pieces of debris in orbit to identify the top fifty most statistically concerning pieces of debris based on conjunction risk [20]. Small debris is considered for removal as well. Since small debris is much more variable than larger debris, this study considered a subset of identified small debris. This thesis considers all small debris with radar cross-sections of less than 0.1 m^2 for which two-line element sets are currently available. This set is filtered to deselect pieces of debris likely to deorbit themselves and group pieces of debris with highly similar orbits. This set of small debris is considered for removal in addition to McKnight et al.'s fifty identified large debris.

The nominal concept of operations of the ADR vehicle obey the following steps. The ADR Vehicle launches to an initial piece of debris for removal. The ADR Vehicle then completes the debris removal, using a predetermined removal method, deploying the appropriate removal payload for the selected debris size. The ADR Vehicle stays in the vicinity of the debris to be removed for the duration of the removal period. After successful removal, the ADR Vehicle travels to the subsequent debris during the travel time. The ADR Vehicle then removes the subsequent debris and travels to the following debris after that. This process continues until the mission is terminated or all debris is removed. This concept of operations is formulated as a MILP and enforced through a set of constraints and an objective function to be solved by the optimizer.

The rest of this thesis is organized as follows. Section 2 presents the modeling of the considered debris and the modeling of the proposed mission. Section 3 describes the developed methods to optimize the ADR mission. Section 4 demonstrates the value of the presented methods for several case studies considering removing variable amounts of debris per year. Finally, Section 5 concludes the thesis.

CHAPTER 2

MODELING AND NETWORK OVERVIEW

This section presents the assumptions for the ADR Vehicle and debris removal devices, the modeling of the debris removal, and the debris considered in the optimization.

2.1 ADR Vehicle and Debris Removal Device High-Level CONOPS

The ADR Vehicle consists of one spacecraft that travels from debris to debris, deploying some debris removal mechanism at each piece of debris. The mission was initially formulated to represent an ADR Vehicle that deploys a guided intercept vehicle to remove large debris and a space sweeper to remove small debris. However, alternate removal strategies could also work as long as they follow the same basic concept of operations. Alternate removal strategies include attaching a deorbiting kit with a propellant capable of modifying the debris' orbit, having the ADR Vehicle manually deorbit each piece of debris, and deploying a space laser to eliminate a set of smaller debris. When the ADR Vehicle comes into close proximity to the targeted debris, it will deploy the appropriate removal method. The high-level concept of operations (CONOPS) for the mission will proceed as follows:

1. The ADR Vehicle and c_{ad} debris removal devices for large debris and c_{be} debris removal devices for small debris are launched from Earth to the first debris for removal.

2. Once sufficiently close to the debris, the ADR Vehicle releases d debris removal devices.

3. After the ADR Vehicle releases the debris removal devices, the debris removal devices are responsible for close-range terminal maneuvering.

4. The ADR Vehicle will stay the same distance around the debris for the duration of the removal, Δt_h.

5. The debris removal devices do not return to the ADR Vehicle. After the debris removal devices complete the removal, the ADR Vehicle either:

   (a) Travels to the next piece of debris, taking q time.

   (b) Stays at the same node for an additional time period until an optimal opportunity arises, if multiple options are defined for q.

6. The ADR Vehicle continues steps 2–5 until all pieces of debris are removed, the ADR Vehicle runs out of debris removal devices, or the mission is terminated.

2.2 ADR Vehicle and Debris Removal Device Assumptions

This high-level concept of operations utilizes several assumptions. First, the debris removal devices can only be deployed at a reasonably close distance from the debris. This requirement is due to the assumption that the ADR Vehicle will maintain a majority of the remote sensing capabilities and terminal maneuvering capabilities for the system. The ADR Vehicle will be responsible for most transportation and maneuvering to the targeted debris. The debris removal devices shall only be responsible for close-range terminal maneuvering around the targeted debris.

Next, all debris considered for removal shall be identified prior to the start of the mission, and the orbital elements and starting locations for all considered debris and debris groups are known. The optimization scheme used to optimize the logistics of this mission is deterministic and requires a known input set of debris. For this reason, all considered debris shall be known before the start of the mission, and the optimized concept of operations and sequence of debris removal will be determined before the launch of the ADR Vehicle.

The debris removal devices are broken down into two groups: large debris removal devices and small debris removal devices. Large debris removal devices are modeled as one device which is capable of removing one large piece of debris within the range of 800–9,000 kg. This range was chosen to include all debris within the set identified by McKnight et al. [20].

The second group of debris removal devices is devices that target small debris. Although the deployment of these devices is identical to the deployment of large debris removal devices, these devices shall be capable of removing all small debris within similar orbits. The concept for these devices is based on proposed space sweeper missions that may target many microdebris over a period of months or years [6, 21, 22]. It is assumed that the space sweeper modeled in this mission can reach all debris with altitudes within $\pm$ 100 km, inclinations within $\pm$ 5°, and RAANs within $\pm$ 5° of the sweeper's operation for an operating time of one year. Additionally, all maneuvering of the debris removal device after deployment is the responsibility of the debris removal device; the ADR Vehicle is only responsible for maneuvering the debris removal device to an ideal orbit for maximum debris removal.

All debris removal devices, regardless of targeted debris size, will be deployed from the same distance from the debris. Additionally, all debris removal devices will take the same amount of time to deploy and require the ADR Vehicle to stay at the targeted debris for the same amount of time, Δt_h.

Within the given orbital maneuver time Δt_t, the actual time length of the maneuver may vary based on the optimal lowest-cost maneuver. However, the ADR Vehicle will not initiate the removal of the debris by deploying a debris removal device until Δt_t is completed. Likewise, since the same amount of time is allotted for removal by each debris removal device, the ADR Vehicle will remain near the debris removal device and debris for the entirety of the debris removal period. After this time period Δt_h has been completed, the ADR Vehicle may travel to the next piece of debris. Within the time-expanded network, an identical amount of time is allotted for each orbital maneuver from one debris to the next and for the removal of debris. The time-expanded network's construction requires this to construct the model as a MILP.

2.3 Considered Debris

Because of the extremely large amount of debris currently orbiting Earth, a subset of debris are prioritized for removal.

2.3.1 Large Debris

McKnight et al. [20] analyzed large pieces of debris to comprise a set of fifty pieces of debris that posed the greatest risk to other objects in low Earth orbit. This set of space debris, consisting primarily of used rocket bodies and defunct satellites, poses the most significant risk to current and future operational satellites and space missions. Therefore, this set of debris should be prioritized for removal.

For each piece of large debris, a reward for removal is assigned. The values of the rewards are based on the benefits identified by Colvin et al. [6]. In this paper, they estimated that removing all fifty debris recognized by McKnight et al. would produce a benefit of $3.5 million in the first year after removal. This value is based on an expected reduction in risk, especially for reducing the probability of debris-on-debris collisions. This total reward is distributed uniformly among all large debris. The reward for each piece of debris in this set is estimated to be $70,000.

All these debris have known orbital elements that are obtainable from satellite tracking services. Many targeted debris have similar inclinations and altitudes, simplifying the required orbital maneuvers to travel from one debris to the next. Additionally, none of this debris is likely to deorbit without intervention in the near future. Therefore, this debris set is considered for removal by the large debris removal devices during the mission.

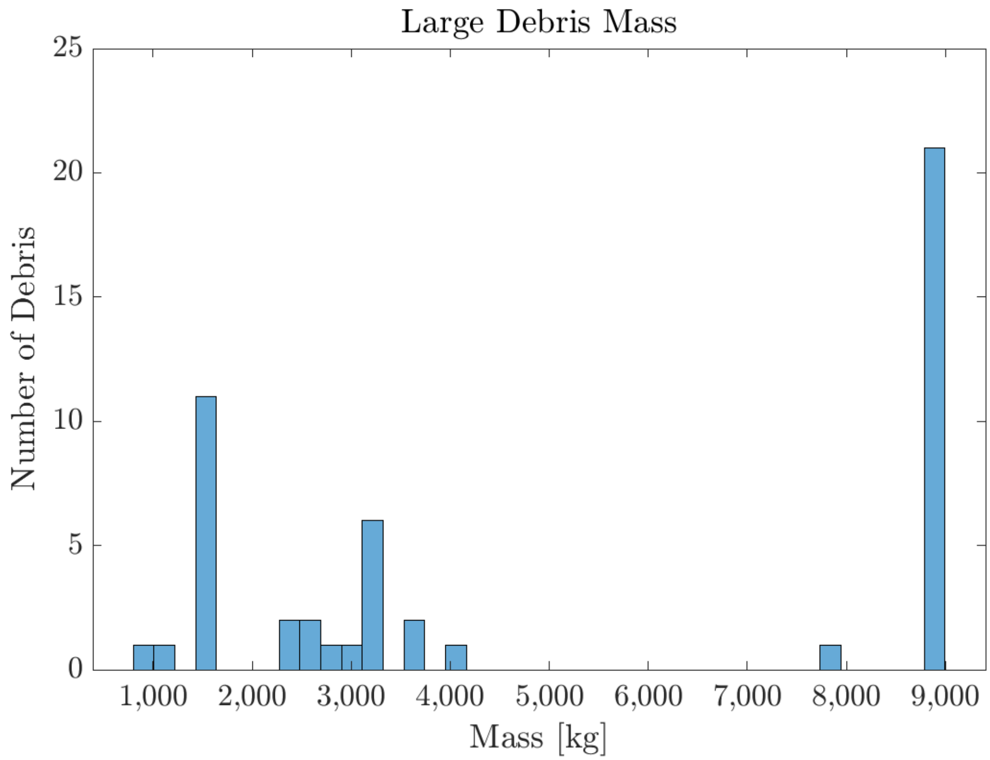

Figure 2.1: Mass distribution of considered large debris

2.3.2 Small Debris

Due to the challenging nature of tracking very small debris, several assumptions were made to simplify the considered small debris set. Small debris tends to have more unstable orbits with less precise orbit determination, and they tend to consist primarily of fragments of larger debris [6]. However, their small mass and size does not eliminate their potential damage to sensitive spacecraft and missions [23].

There are tens of thousands of untrackable pieces of small debris orbiting the Earth today. To consider a smaller number of potential debris for removal, this thesis considers small debris for which there are two-line element sets available. To obtain this set of small debris, Space-Track.org was queried for all currently tracked debris objects. This set was filtered to only include debris with a radio cross section of less than 0.1 m^2. This query returned 9,567 pieces of debris.

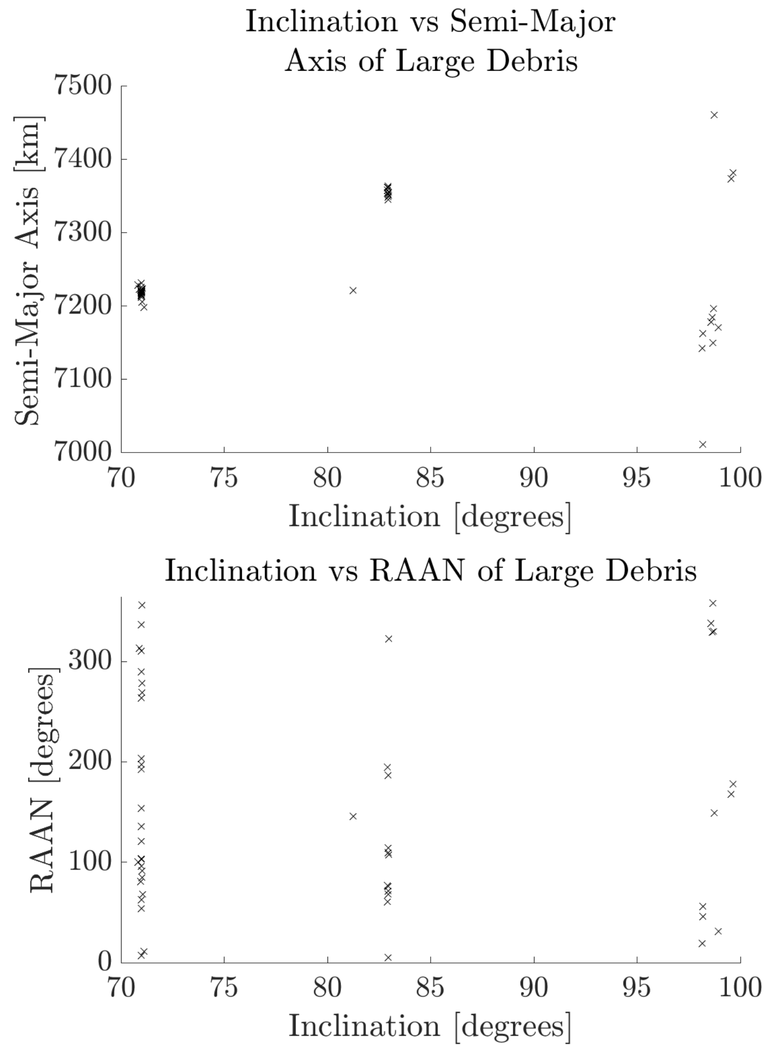

Figure 2.2: Orbital element clusters of large debris

Out of the 9,567 small debris initially identified for removal, each debris was propagated forward for a period of ten years using SGP4 to identify if the debris is likely to decay on its own. Out of 9,567 initially considered debris, 2,097 debris are likely to decay on their own within the next ten years. This debris was removed from the data set of considered small debris.

Based on the assumption that a deployed small debris removal device would resemble a space sweeper and be capable of removing all debris within a certain altitude, inclination range, and RAAN range, the remaining debris was grouped within similar altitude, inclination, and RAAN ranges. The ranges for allowable orbital elements for potential removal by one small debris removal device were chosen based on reasonable assumptions for theoretical space sweepers. All debris with orbital elements within this range is grouped, as one sweeper may handle all of this debris.

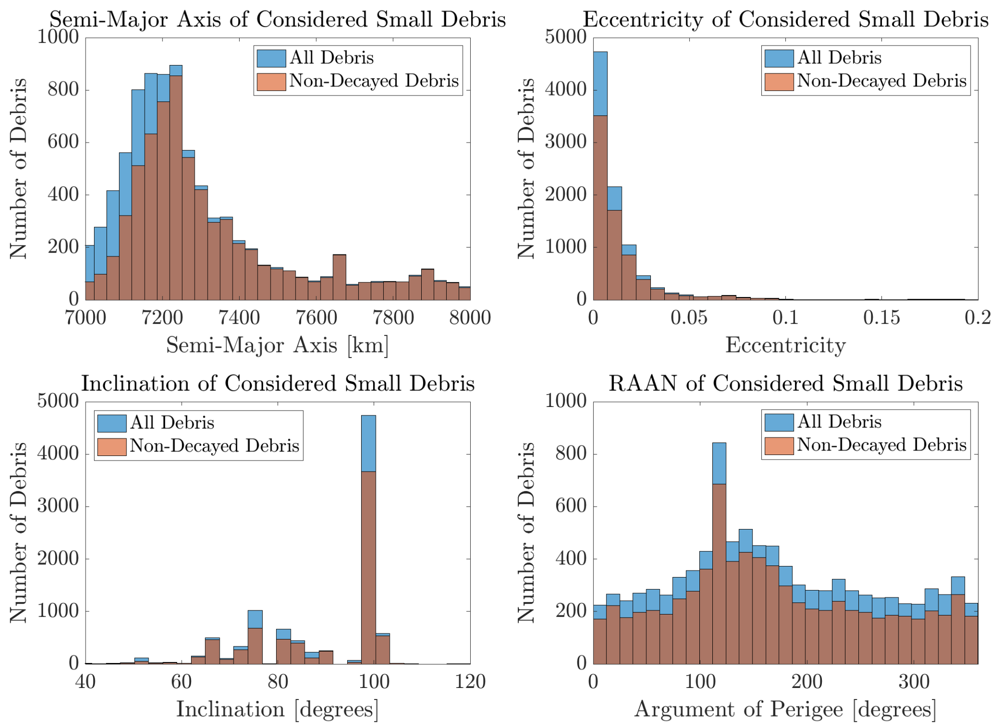

Figure 2.3: Distribution of orbital elements for all considered and non-decayed small debris

Table 2.1: Allowable orbital element ranges for removal by one small debris removal device

Orbital Element	**Range for Removal**
Semi-Major Axis Range	$\pm$ 100 km
Inclination Range	$\pm$ 5°
RAAN Range	$\pm$ 5°

These groupings produced 1,468 unique groups of debris. A vast majority of these groups had fewer than fifty debris in each group. It would not be practical to deploy a debris removal device to remove fewer than 100 small debris in one group. For that reason, groups of small debris with fewer than 100 debris were filtered out of the data set.

These parameters produced five groups of small debris that could each be removed by one deployed space sweeper-type device over one year. In the data set of considered debris, each group of small debris with similar orbits is treated as one debris, with reward weightings appropriate for the number of debris in that group. Representative two-line element sets for each group of small debris were then added to the set of fifty large debris considered for removal.

Rewards for each group of small debris were assigned similarly to award assignments for large debris. Based on Colvin et al.'s cost-benefit analysis, [6] there is an estimated benefit totaling $23 million after one year for removing 100,000 pieces of small debris. This amount is also based on potential damage to the LEO environment if this debris is left unmediated. If the total benefit for removing 100,000 pieces of debris is $23 million, then the approximate benefit for removing each piece of debris is $230. For the considered small debris, the total obtainable reward for removing all debris is approximately $233,910. Multiplying $230 by the number of debris in the group produces the approximate reward for the removal of each entire group of small debris.

It is worth noting that the distribution of the debris groupings is not uniform. Many pieces of debris could have been assigned to at least two groups of debris since their inclination and semi-major axis fall within the allowable ranges of those groups. The algorithm used to group the debris did not take into account distributing debris over groups evenly. Contrarily, the algorithm assigned a given small piece of debris to the first matching group it found by iterating over a list. Regrouping the debris set differently would assign different costs to each debris group and produce slightly different results and optimal missions. However, in the case of the presented data set, Group 1 had significantly more pieces of debris than the other groups with 341 pieces of debris, which were all able to be entirely removed by one deployed small debris removal device.

Table 2.2: Small debris groupings

Group Number	**Semi-Major Axis Range**	**Inclination Range**	**RAAN Range**	**Number of Debris**	**Reward**
1	7247.21 $\pm$ 100 km	99.90 $\pm$ 5°	112.40 $\pm$ 5°	341	$78,430
2	7247.61 $\pm$ 100 km	99.90 $\pm$ 5°	122.10 $\pm$ 5°	219	$50,370
3	7245.94 $\pm$ 100 km	100.03 $\pm$ 5°	130.93 $\pm$ 5°	186	$42,780
4	7196.92 $\pm$ 100 km	99.96 $\pm$ 5°	172.77 $\pm$ 5°	146	$33,580
5	7309.94 $\pm$ 100 km	99.53 $\pm$ 5°	149.88 $\pm$ 5°	125	$28,750

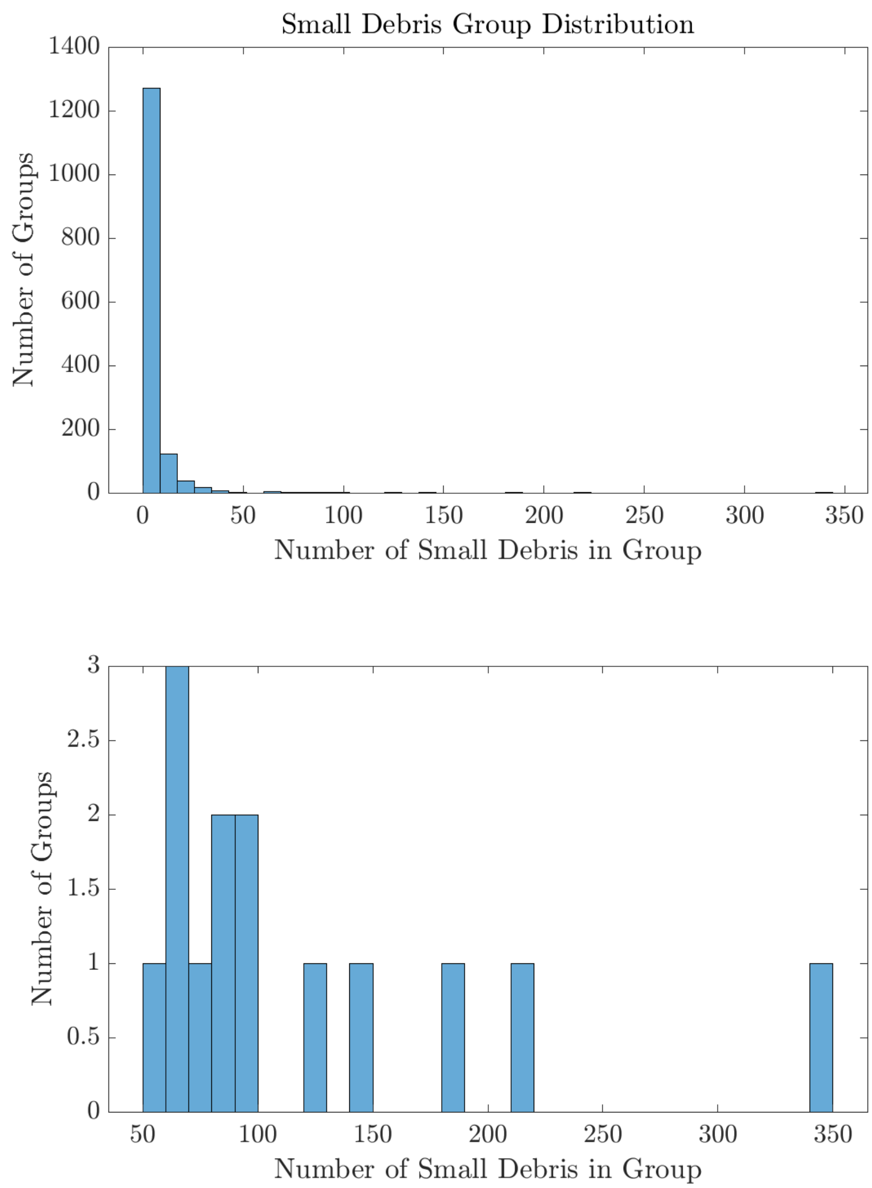

Figure 2.4: Distribution of number of small debris in each group

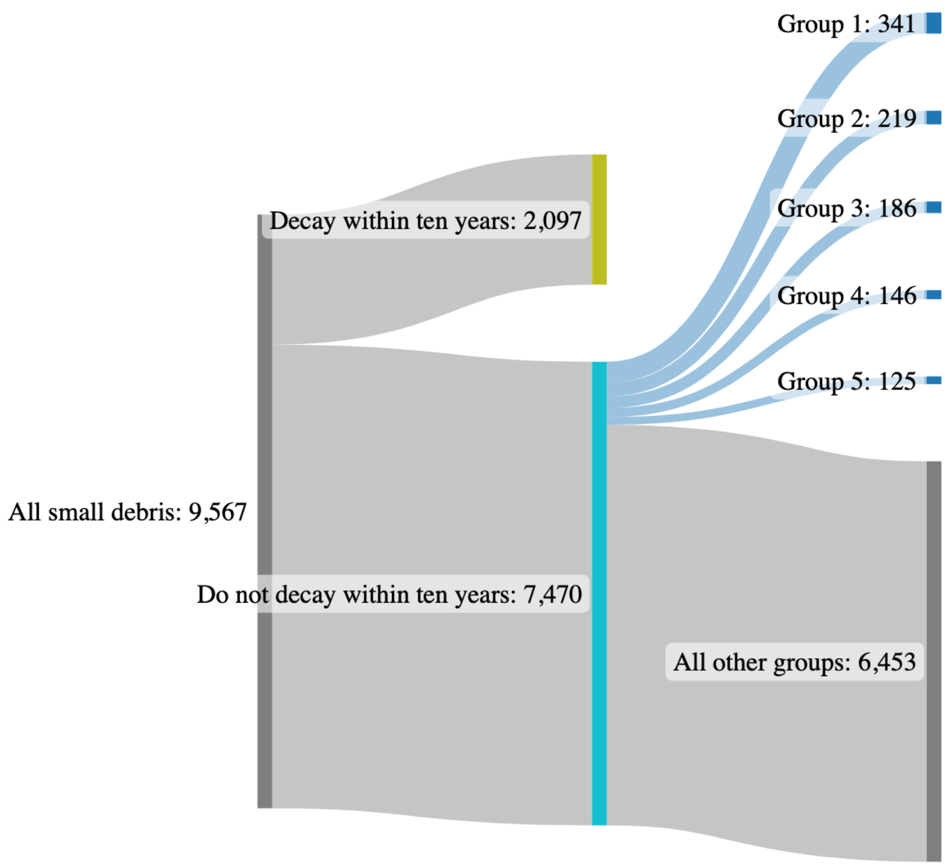

Figure 2.5: Selected and deselected small debris

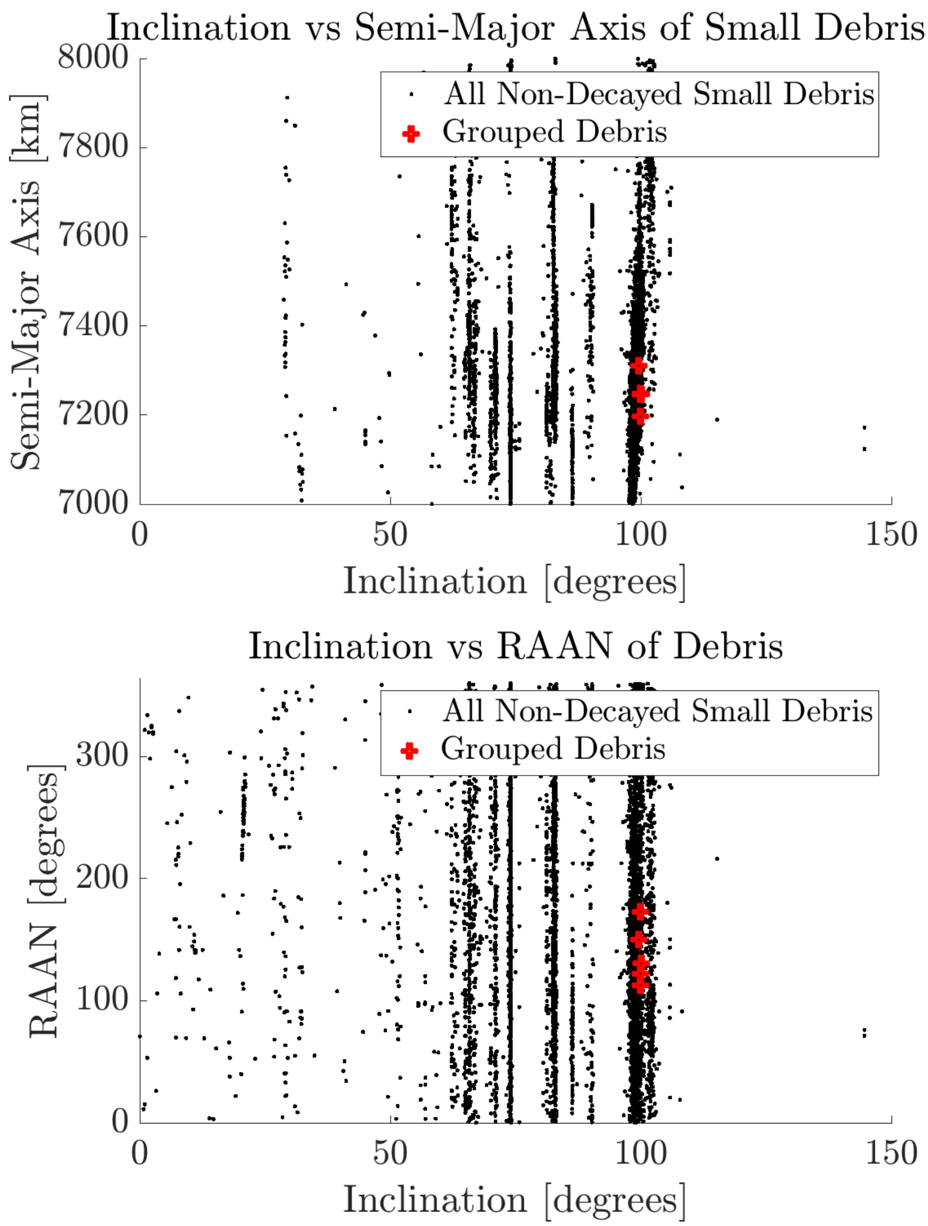

Figure 2.6: Orbital element clusters of small debris

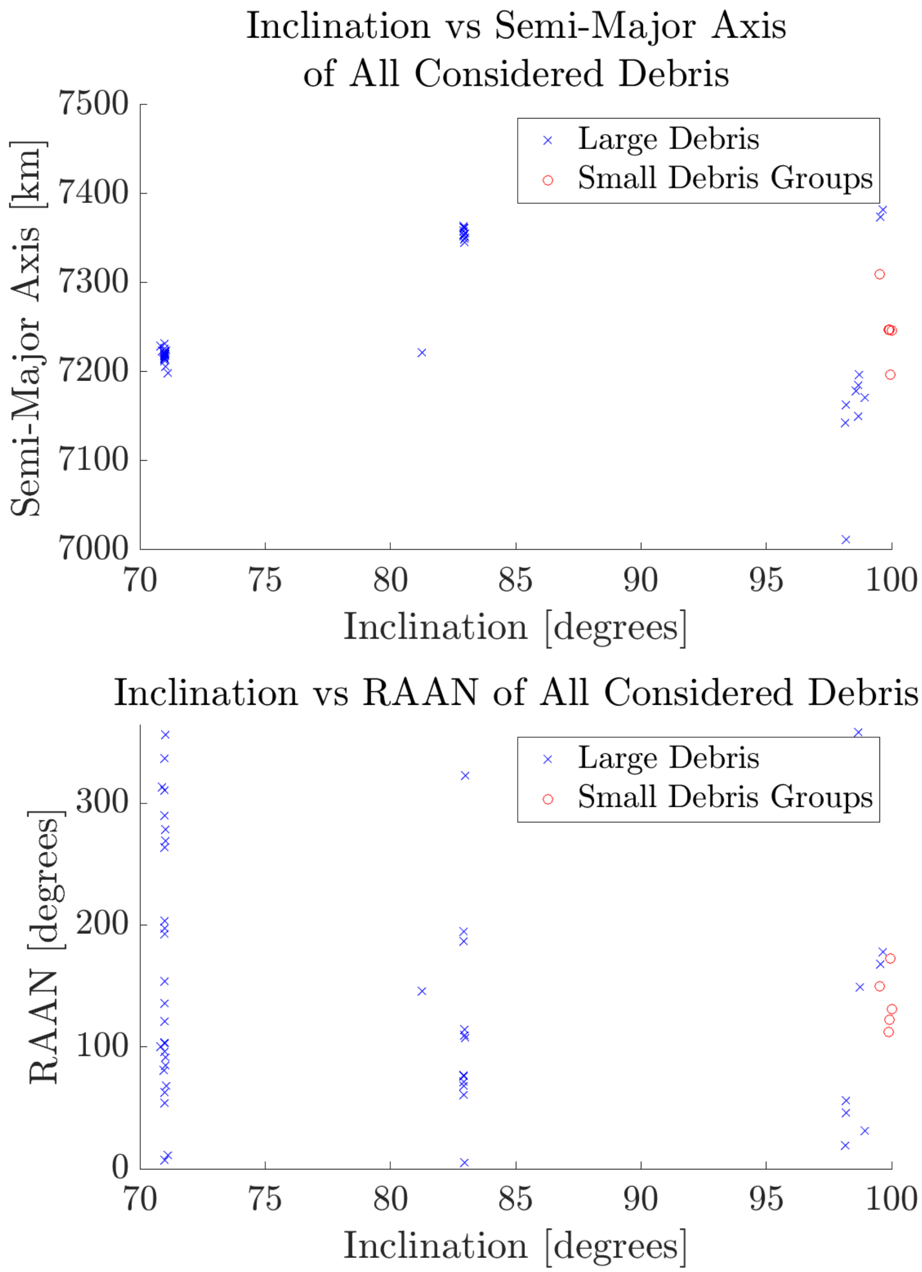

Figure 2.7: Orbital element clusters of all large debris and small debris groups in debris data set

CHAPTER 3
METHODS

This section introduces the methods used to optimize the ADR mission. Section 3.1 describes the trajectory modeling used to estimate orbital maneuvers from each debris to the next for the ADR Vehicle. Section 3.2 introduces the dual objectives that the optimization framework seeks to minimize. Section 3.3 describes how the most efficient mission is determined from a set of potential high-reward missions. Section 3.4 describes how the network is expanded over time using a time-expanded network. Section 3.5 presents the space logistics formulation and how it models the ADR Vehicle operations.

3.1 Trajectory Model

The optimization framework involves trajectory modeling to calculate the ΔV and propellant required to travel from one debris to another for each possible debris pair and time step in the time-expanded network. The outputs of the trajectory model contain the required ΔV for each possible maneuver between debris and are later used in the ADR logistics formulation.

The trajectory of the ADR Vehicle from one debris to the next is modeled as a two-impulse high-thrust maneuver. A grid search is used to find the maneuver that requires the lowest amount of ΔV within an allowable amount of time Δt_t. Within a set period of time Δt_t, Lambert's problem is solved for all potential departure and arrival times and each possible number of revolutions. The grid search returns the smallest ΔV for the lowest-cost maneuver from the set of possible maneuvers satisfying the ADR Vehicle's travel constraints. The position of each debris is propagated for each start and stop time using SGP4 [24]. The multi-revolution Lambert's problem for each possible combination of parameters is solved with ESA's Pykep module using the routine introduced by Izzo

[25, 26]. Each debris is propagated using a high-fidelity method considering nonspherical effects, drag, and other potential orbit perturbations. However, for orbital maneuvers, the transfer time is assumed to be small enough so that orbit perturbations may be neglected. The multi-revolution Lambert algorithm combined with this grid search approach enables evaluation of the lowest-cost trajectory within the allowed time period.

Figure 3.1 demonstrates the algorithm for the trajectory model grid search. Figure 3.2 demonstrates example results for a grid search exploring departure and arrival times between two rocket bodies occupying similar orbits regarding inclination and altitude. This example begins searching on a departure date of March 18, 2021, and explores all arrival and departure times between one and fifty days after that and up to 1,000 revolutions. In this case, the lowest found ΔV is 0.068 km/s, which occurs at t_0 = 36 and t_f = 48, with a time of flight of 12 days. For the presented results in Chapter 4, the grid search explored 20 possible start times, 20 possible end times, and up to 1,000 revolutions.

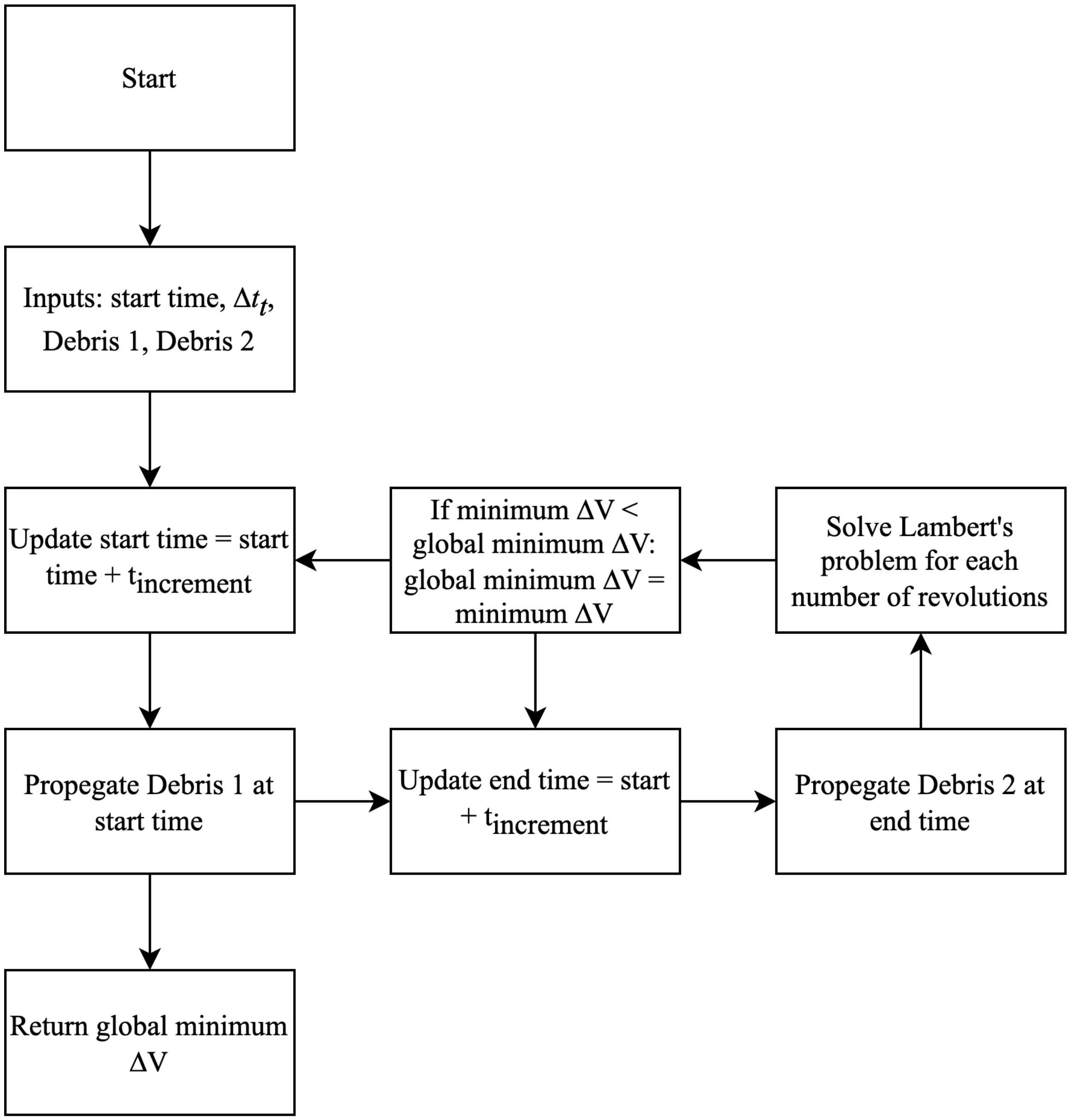

Figure 3.1: Algorithm for trajectory model grid search

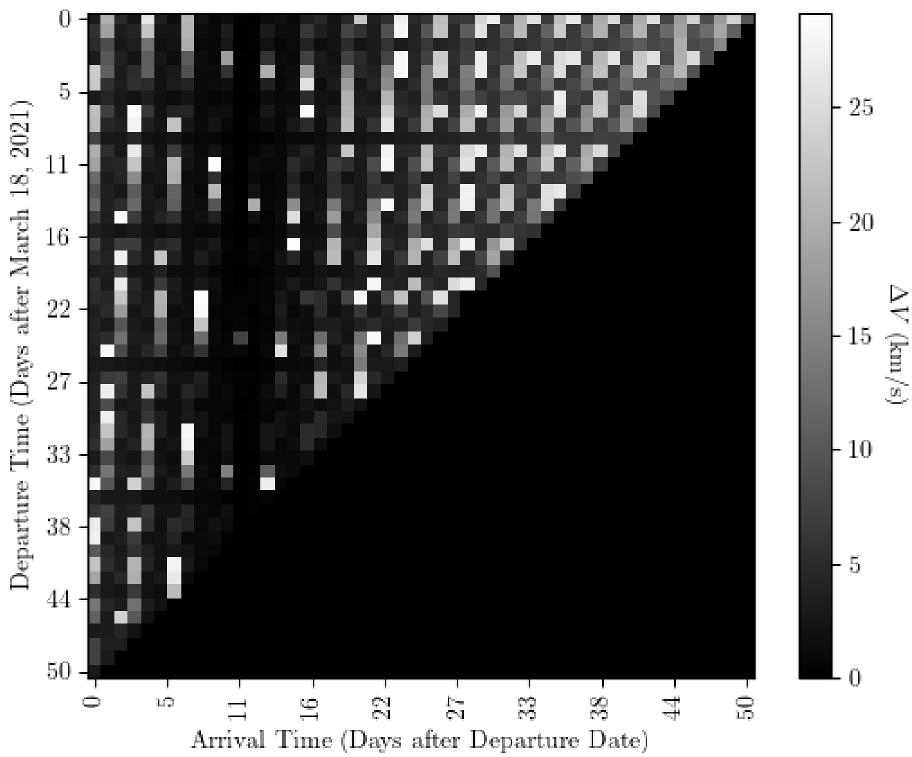

Figure 3.2: ΔV for different departure and arrival combinations for an example maneuver

3.2 Optimization Objectives

Given a set of mission constraints, finding a concept of operations that satisfies the minimum number of desired debris to be removed, maximizes the available reward over the mission, and minimizes the propellant required to obtain this reward is desirable.

The total obtainable reward for the given debris set monotonically increases with propellant capacity. Since many pieces of debris have identical large rewards, when the maximum reward for removing the desired number of debris has been achieved, the obtainable reward plateaus as propellant capacity increases. Figure 3.3 demonstrates this concept. A solution that obtains the maximum reward may not necessarily require the lowest ΔV and propellant to obtain this reward. Any sequence of a selected subset of debris to remove will produce an identical reward. There may be an alternate subset or sequence of debris to remove that may produce a lower-cost mission. Finding the lowest-cost mission that maximizes reward is desirable.

The objective of the presented formulation is to optimize the mission for two objectives: to minimize the propellant required to obtain the maximum possible reward over the mission duration. In Figure 3.3, this solution is represented by the red point. This objective is achieved by iteratively updating the provided ADR Vehicle propellant capacity through a binary search and solving a MILP representing the ADR Vehicle's logistics at each iteration. The binary search is described in Section 3.3, while the logistics formulation is described in Section 3.5.

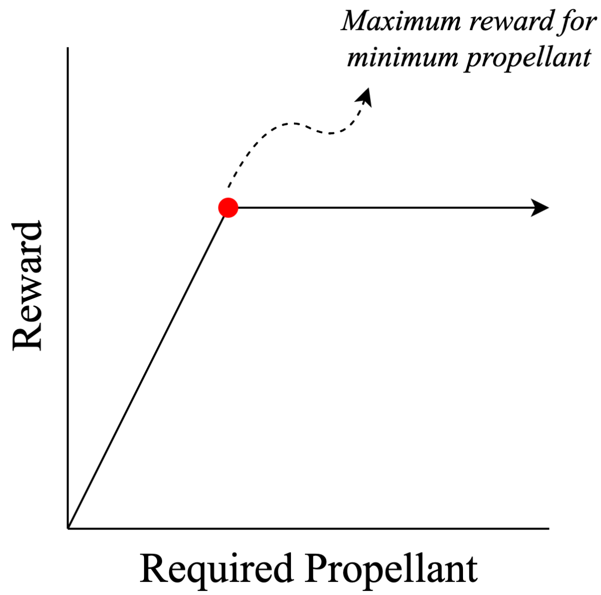

Figure 3.3: Obtainable reward versus required propellant for debris removals

3.3 Binary Search Algorithm

To find the lowest-cost mission that still maximizes reward, a binary search finds the lowest possible propellant capacity that achieves the maximum reward. The algorithm is designed to find the solution with the maximum reward obtained from the formulation in Section 3.5 while minimizing the mission's required ΔV and propellant. The constraints describing the ADR Vehicle's propellant capacity (described below in Equation 3.2 and Equation 3.3) can be leveraged to iteratively update the propellant capacity until a minimum ΔV is found.

Given an initial guess for a range that the solution may be in, indicated by $m_{p,\text{max}}$, the maximum propellant, and $m_{p,\text{min}}$, the minimum propellant, the algorithm splits the range of propellant values into two and recursively searches for the maximum reward on each side of the midpoint. The algorithm solves the MILP with the updated propellant capacity to obtain the maximum reward for the mission. If the optimizer returns a solution with a reward that is less than the maximum obtainable reward, the search range is constrained, with the minimum propellant being set to the midpoint. If the optimization returns a reward that is equal to the maximum determined reward, the search range is updated with the maximum propellant being set to the midpoint. The entire process then repeats until the propellant range is within some tolerance. The search will eventually converge to the solution if the optimal propellant capacity to obtain the maximum possible reward exists within the maximum and minimum propellant values.

The algorithm has a time complexity of $O(\log n)$, where n is the range of propellant values. The algorithm uses a binary search approach to find the solution, which halves the search space with each recursive call.

Table 3.1: Description of the binary search algorithm

Step	**Task Description**
Step 1	Given some maximum propellant $m_{p,\text{max}}$ and minimum propellant $m_{p,\text{min}}$, divide the search space into two by its midpoint, m_p.
Step 2	Optimize the MILP, setting c_{zw}= m_p.
Step 3	If the obtained reward is greater than or equal to the maximum obtainable reward, set $m_{p,\text{max}} = m_p$. If the obtained reward is less than the maximum obtainable reward, set $m_{p,\text{min}} = m_p$.
Step 4	Return to Step 2. Repeat Steps 2-3 until $\lvert m_{p,\text{max}} - m_{p,\text{min}} \rvert <$ tolerance.

3.4 Time-Expanded Network

One can model the ADR Vehicle's operations over a discretized time period by replicating the static debris removal logistics network over a set of predefined time steps. The time-expanded network comprises several parameters defining the network over each static network node. These parameters include the time step for traveling from one debris to another, Δt_t, and the time step during which debris removal occurs, Δt_h. The logistics are formulated so that the ADR Vehicle must travel from one debris to the next over the time period Δt_t. The actual length of the maneuver may take less time than Δt_t; however, the ADR Vehicle must remain at the following debris for the remaining duration of the time period and may not begin debris removal until this time period has passed. Next, Δt_h is allotted for debris removal. Similarly, the ADR Vehicle must remain in the vicinity of the debris to be removed for the entire duration of the time step. Only after this time period has elapsed can the ADR Vehicle travel to the next piece of debris.

The parameter Δt is the sum of Δt_h and Δt_t. The length of Δt will determine the coarseness of the time-expanded network. The static network, including all debris, all debris removal devices, and the ADR Vehicle, is defined at each node of the time-expanded network. The network is defined for each time step Δt_t and Δt_h for a total length of T, which is the maximum length of the mission. For instance, consider a mission with a total length of 300 days. The chosen length of Δt_t may be 45 days and the chosen length of Δt_h may be 5 days, so Δt will be 50 days. In this case, the maximum number of pieces of debris removed over the entire period will be six.

It is possible to vary the time discretization. For instance, a very short time discretization will result in a considerable optimization time. Alternatively, a large time discretization will result in a faster optimization time while sacrificing results accuracy. The number of variables increases with the number of time steps within the time-expanded network.

Figure 3.4 depicts how each time step replicates each element of the static network. For each node, the static network including the ADR Vehicle, debris removal devices, and all debris is modeled.

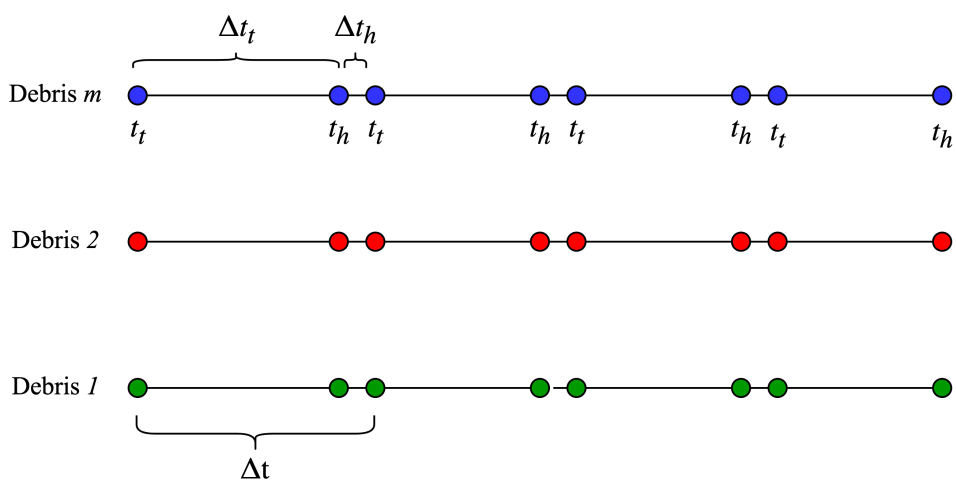

Figure 3.4: Simplified time-expanded network

3.5 Logistics Formulation

This subsection introduces the mathematical logistics optimization formulation. In particular, we introduce the logistics formulation used for the subsequent modeling and optimization of the dynamic traveling salesperson problem. The objective of the logistics formulation is to 1) accurately model the ADR Vehicle logistics over the time dimension, 2) formulate the ADR mission as a MILP with a global optimum that is obtainable, and 3) determine the optimal, maximum-reward concept of operations and order of debris removal for the ADR Vehicle.

3.5.1 Index Sets

The time-expanded network consists of a set of nodes $\mathcal{N}$ consisting of $\mathcal{N}_p$ and $\mathcal{N}_d$. $\mathcal{N}_p$ contains the set of start nodes, or the node that the ADR Vehicle begins the timeline at. $\mathcal{N}_p$ is a functionally arbitrary point that handles initial conditions and each variable's behavior at the mission's beginning. The ΔV and propellant required to travel from $\mathcal{N}_p$ to any debris node in $\mathcal{N}_d$ equal zero, and the start node does not affect the optimization results.

$\mathcal{N}_d$ contains the set of debris nodes, or all the debris considered in the problem. These nodes are defined at every time step within $\mathcal{T}$, and connected by transportation arcs, connecting nodes to each other, and holdover arcs, which connect a node to itself at a later time step. The set $\mathcal{N}$ of debris nodes is categorized into two subsets of debris nodes: set $\mathcal{N}_{dl}$ and set $\mathcal{N}_{ds}$. $\mathcal{N}_{dl}$ represents all large debris nodes, while $\mathcal{N}_{ds}$ represents all small debris nodes. Debris nodes are assigned to $\mathcal{N}_{dl}$ and $\mathcal{N}_{ds}$ based on their mass. Each transportation arc has an index (i, j), meaning that the ADR Vehicle flies from node i to node j. Each holdover arc has an index i.

$\mathcal{T}$ contains the set of time steps that are defined in the time-expanded network. $\mathcal{T}$ consists of $\mathcal{T}_t$ and $\mathcal{T}_h$, which contain the set of travel time steps and holdover time steps, respectively. The ADR Vehicle must remove debris only during a time step in $\mathcal{T}_h$, and it must travel between debris only during a time step in $\mathcal{T}_t$.

Lastly, $\mathcal{Q}$ defines the time of flight options that the ADR Vehicle may take to go from one debris node to another. If only one option is defined within $\mathcal{Q}$, then the ADR Vehicle must travel over the same amount of time each time, but if multiple options are defined, then the ADR Vehicle may remain at a debris node for a greater period of time after removal and travel to the next debris node during a different time step. These index sets are summarized in Table 3.2.

Table 3.2: Definition of the index sets appearing in the logistics formulation

Index Sets	
$\mathcal{N}$	All debris nodes and start node (i, j)
$\mathcal{N}_p$	All start nodes (i, j) in $\mathcal{N}$
$\mathcal{N}_d$	All debris nodes (i, j) in $\mathcal{N}$
$\mathcal{N}_{ds}$	All small debris nodes (i, j) in $\mathcal{N}$
$\mathcal{N}_{dl}$	All large debris nodes (i, j) in $\mathcal{N}$
$\mathcal{T}$	The set of time steps
$\mathcal{T}_t$	The set of time steps followed by Δt_t
$\mathcal{T}_h$	The set of time steps followed byΔt_h
$\mathcal{Q}$	The set of time of flight maneuvers

3.5.2 Variables

Each variable defined in Table 3.3 describes the behaviors of the ADR Vehicle, debris removal devices, and propellant over the time-expanded network. Different index sets are defined for the holdover or transportation arcs, and these variables are defined for the index sets described in Section 3.5.1. For each holdover arc, the variable is defined for all t in $\mathcal{T}_h$, and for each node n in $\mathcal{N}$. For each transportation arc, the variable is defined for all i, j in $\mathcal{N}$, where the arc travels from i to j. The variable is also defined for all t in the set of time steps $\mathcal{T}_t$, and for each time of flight option q in $\mathcal{Q}$.

The binary variables X_{it} and U_{ijtq} represent the ADR Vehicle, which indicate the presence of the ADR Vehicle at a node i in the time-expanded network at time t. The set of debris removal devices is separated by the size of the pieces of debris they can remove.

The variables A_{it} and D_{ijtq} represent the set of small debris removal devices. The variables B_{it} and E_{ijtq} represent the set of large debris removal devices. Each variable for both the small debris removal devices and the large debris removal devices can be any natural number. These indicate the remaining debris removal devices of each type onboard the ADR Vehicle and the number of debris removal devices deployed at the appropriate debris node.

Propellant is represented by $Z_{it}^{\pm}$ and $W_{ijtq}^{\pm}$ for the holdover and transportation arcs, respectively. These variables may take on any real number and represent the amount of propellant onboard the ADR Vehicle and the propellant expenditure over a transportation arc. The superscript $+$ or $-$ indicates whether the variable is defined before or after a time step. Lastly, H_{it} is a binary service variable that represents the presence of the ADR Vehicle at a node in $\mathcal{N}$.

Table 3.3: Definition of the variables appearing in the logistics formulation

	Holdover Arcs	Transportation Arcs
Flow Variables	$i \in \mathcal{N}, t \in \mathcal{T}_h$	$i, j \in \mathcal{N}, i \neq j, t \in \mathcal{T}_t, q \in \mathcal{Q}$
ADR Vehicle	$X_{it} \in \{0, 1\}$	$U_{ijtq} \in \{0, 1\}$
Small Debris Removal Device	$A_{it} \in \mathbb{N}$	$D_{ijtq} \in \mathbb{N}$
Large Debris Removal Device	$B_{it} \in \mathbb{N}$	$E_{ijtq} \in \mathbb{N}$
Propellant	$Z_{it}^{\pm} \in \mathbb{R}^{+} \cup \{0\}$	$W_{ijtq}^{\pm} \in \mathbb{R}^{+} \cup \{0\}$
Service Variables	$H_{it} \in \{0, 1\}$	

3.5.3 Parameters

Table 3.4 outlines the mission parameters that describe the ADR Vehicle's logistics and behavior over the mission. Each parameter provides information about the mission's requirements, the ADR Vehicle's capacity, the discretization of the time-expanded network, the mass of each component of the ADR Vehicle, and the necessary values for modeling the propellant expenditure during each orbital maneuver.

Table 3.4: Definition of the parameters appearing in the logistics formulation

ψ	The minimum desired number of debris for removal
w_{it}	The reward for removing debris i at time t
c_{zw}	The propellant capacity of the ADR Vehicle
c_{ad}	The small debris removal device capacity of the ADR Vehicle
c_{be}	The large debris removal device capacity of the ADR Vehicle
Δt	A period of time in the time-expanded network
Δt_h	Length of the debris removal portion of Δt
Δt_t	Length of the travel portion of Δt
m_{ADRV}	Structural mass of the ADR Vehicle
$m_{DRD,\text{Small}}$	Mass of one small debris removal device
$m_{DRD,\text{Large}}$	Mass of one large debris removal device
r_{ijtq}	Propellant consumption factor
ΔV_{ijtq}	ΔV for a high-thrust ADR Vehicle to travel from i to j in q time starting from time step t
g_0	Gravitational acceleration
I_{sp}	Specific impulse
d	Number of debris removal devices deployed at a debris node

3.5.4 Objective Function

The objective function seeks to maximize the total reward obtained from removing debris throughout the mission. It summates the reward associated with removing debris i at time t, w_{it}, over all debris nodes $\mathcal{N}_d$ and all removal time steps $\mathcal{T}_h$.

$$J = \sum_{i \in \mathcal{N}_d} \sum_{t \in \mathcal{T}_h} w_{it} H_{it} \tag{3.1}$$

3.5.5 Constraints

Lastly, the optimizer considers a set of constraints to finish defining the mission logistics. The constraints are grouped into four categories: capacity constraints, transformation constraints, mass balance constraints, and operational constraints.

Capacity Constraints

The capacity constraints are defined in Equations 3.2, 3.3, 3.4, 3.5, 3.6, and 3.7, and enforce that the ADR Vehicle may not have more propellant than its defined propellant capacity and may not have more debris removal devices than its defined debris removal device capacity. Equations 3.2 and 3.3 correspond to propellant, and Equations 3.4, 3.5, 3.6, and 3.7 correspond to debris removal devices.

$$\forall i \in \mathcal{N}, \forall t \in \mathcal{T}_h : \qquad Z^+_{it} \leq c_{zw} X_{it} \tag{3.2}$$

$$\forall i, j \in \mathcal{N}, i \neq j, \forall t \in \mathcal{T}_t, \forall q \in \mathcal{Q} : \qquad W^+_{ijtq} \leq c_{zw} U_{ijtq} \tag{3.3}$$

$$\forall i \in \mathcal{N}, \forall t \in \mathcal{T}_h : \qquad A_{it} \leq c_{ad} X_{it} \tag{3.4}$$

$$\forall i \in \mathcal{N}, \forall t \in \mathcal{T}_h : \qquad B_{it} \leq c_{be} X_{it} \tag{3.5}$$

$$\forall i, j \in \mathcal{N}, i \neq j, \forall t \in \mathcal{T}_t, \forall q \in \mathcal{Q} : \qquad D_{ijtq} \leq c_{ad} U_{ijtq} \tag{3.6}$$

$$\forall i, j \in \mathcal{N}, i \neq j, \forall t \in \mathcal{T}_t, \forall q \in \mathcal{Q} : \qquad E_{ijtq} \leq c_{be} U_{ijtq} \tag{3.7}$$

Transformation Constraints

Equations 3.8 and 3.11 define the transformation constraints for the ADR Vehicle's propellant expenditure over transportation arcs. The trajectory model provides ΔV_{ijtq} for a given beginning node i, ending node j, time t, and time of flight q. Based on ΔV_{ijtq}, the ADR Vehicle's mass including all remaining debris removal devices, and a modified version of the rocket equation, Equation 3.8 describes how propellant is spent over a transportation arc.

$$\forall i, j \in \mathcal{N}, i \neq j, \forall t \in \mathcal{T}_t, \forall q \in \mathcal{Q}: \qquad W^-_{ijtq} = W^+_{ijtq} - r_{ijtq} M_{ijtq} \tag{3.8}$$

$$r_{ijtq} = 1 - \exp\left(\frac{-\Delta V_{ijqt}}{g_0 I_{sp}}\right) \tag{3.9}$$

$$M_{ijtq} = m_{ADRV} U_{ijtq} + W^+_{ijtq} + m_{DRD,\text{Small}} D_{ijtq} + m_{DRD,\text{Large}} E_{ijtq} \tag{3.10}$$

$$\forall i \in \mathcal{N}, \forall t \in \mathcal{T}_h: \qquad Z^-_{it} = Z^+_{it} \tag{3.11}$$

Mass Balance Constraints

The mass balance constraints are defined in Equations 3.12 through 3.19. Equations 3.12, 3.14, 3.16, and 3.17 define the initial conditions for the ADR Vehicle, debris removal devices, and propellant at the beginning of the time-expanded network, setting each variable to the correct value at the start node and beginning time step of the time-expanded network. Equations 3.13, 3.15, 3.18, and 3.19 enforce mass-balance equalities for each variable over each arc in the time-expanded network. Additionally, Equations 3.18 and 3.19 enforce the behavior of the debris removal devices so that they are only deployed at their respective targeted category of debris.

$$X_{i0} = \begin{cases} 1, i \in \mathcal{N}_p \\ 0, i \in \mathcal{N}_d \end{cases} \tag{3.12}$$

$$\forall i \in \mathcal{N}, \forall t \in \mathcal{T}, t > 0: \qquad \sum_{\substack{j \in \mathcal{N} \\ j \neq i \\ q \in \mathcal{Q} \\ t \in \mathcal{T}_t}} U_{ijtq} - \sum_{\substack{j \in \mathcal{N} \\ j \neq i \\ q \in \mathcal{Q} \\ t-q \in \mathcal{T}_t \\ t \in \mathcal{T}_h}} U_{ij(t-q)q} = 0 \tag{3.13}$$

$$Z_{i0}^{+} = \begin{cases} c_{zw} X_{i0}, i \in \mathcal{N}_p \\ 0, i \in \mathcal{N}_d \end{cases} \tag{3.14}$$

$$\forall i \in \mathcal{N}, \forall t \in \mathcal{T}, t > 0 : \quad Z_{it}^{+} - Z_{i(t-\Delta t)}^{-} + \sum_{\substack{j \in \mathcal{N} \\ j \neq i \\ q \in \mathcal{Q} \\ t \in \mathcal{T}_t}} W_{ijtq}^{+} - \sum_{\substack{j \in \mathcal{N} \\ j \neq i \\ q \in \mathcal{Q} \\ t-q \in \mathcal{T}_t \\ t \in \mathcal{T}_h}} W_{ijtq}^{-} = 0 \tag{3.15}$$

$$\forall i \in \mathcal{N} : \qquad A_{i0} = \begin{cases} c_{ad} X_{i0}, i \in \mathcal{N}_p \\ 0, i \in \mathcal{N}_d \end{cases} \tag{3.16}$$

$$\forall i \in \mathcal{N} : \qquad B_{i0} = \begin{cases} c_{be} X_{i0}, i \in \mathcal{N}_p \\ 0, i \in \mathcal{N}_d \end{cases} \tag{3.17}$$

$$\forall i \in \mathcal{N}, \forall t \in \mathcal{T}, t > 0 : A_{it} - A_{i(t-\Delta t)} + \sum_{\substack{j \in \mathcal{N} \\ j \neq i \\ q \in \mathcal{Q} \\ t \in \mathcal{T}_t}} D_{ijtq} - \sum_{\substack{j \in \mathcal{N} \\ j \neq i \\ q \in \mathcal{Q} \\ t \in \mathcal{T}_h \\ t-q \in \mathcal{T}_t}} D_{ij(t-q)q} = \begin{cases} dH_{it}, i \in \mathcal{N}_{ds} \\ 0, i \in \mathcal{N}_p \\ 0, i \in \mathcal{N}_{dl} \end{cases} \tag{3.18}$$

$$\forall i \in \mathcal{N}, \forall t \in \mathcal{T}, t > 0: \quad B_{it} - B_{i(t-\Delta t)} + \sum_{\substack{j \in \mathcal{N} \\ j \neq i \\ q \in \mathcal{Q} \\ t \in \mathcal{T}_t}} E_{ijtq} - \sum_{\substack{j \in \mathcal{N} \\ j \neq i \\ q \in \mathcal{Q} \\ t \in \mathcal{T}_h \\ t-q \in \mathcal{T}_t}} E_{ij(t-q)q} = \begin{cases} dH_{it}, i \in \mathcal{N}_{dl} \\ 0, i \in \mathcal{N}_p \\ 0, i \in \mathcal{N}_{ds} \end{cases} \tag{3.19}$$

Operational Constraints

Lastly, Equations 3.20, 3.21, 3.22, 3.23, and 3.24 define the operational constraints and enforce the desired behaviors of the ADR mission. Equation 3.20 enforces that each node may be visited at a maximum of one time so that the ADR Vehicle does not travel to a debris node that has already been removed. Equation 3.21 states that the ADR Vehicle is initially deployed at the start node prior to removal or travel. Equation 3.22 allows the ADR Vehicle to stay as long as desired at a given node if no optimal path to another node exists yet and multiple time of flight options within $\mathcal{Q}$ are defined. Equation 3.23 prevents the ADR Vehicle from traveling to another node at the end of the timeline. Equation 3.24 requires that the ADR Vehicle removes at least the desired number of debris over the entire timeline. Together with the objective function, these constraints define the logistics formulation as a MILP for the optimizer to solve.

$$\forall i \in \mathcal{N}: \qquad \sum_{t \in \mathcal{T}_h} H_{it} \leq 1 \tag{3.20}$$

$$\forall i \in \mathcal{N}: \qquad H_{i0} = \begin{cases} 1, i \in \mathcal{N}_p \\ 0, i \in \mathcal{N}_d \end{cases} \tag{3.21}$$

$$\forall i \in \mathcal{N}, \forall t \in \mathcal{T}_h, t > 0: \qquad \sum_{\substack{j \in \mathcal{N} \\ j \neq i \\ q \in \mathcal{Q} \\ t-q \in \mathcal{T}_t}} U_{ji(t-q)q} = H_{it} \tag{3.22}$$

$$\forall i \in \mathcal{N}, \forall j \in \mathcal{N}, i \neq j, \forall t \in \mathcal{T}_t, \forall q \in \mathcal{Q}, t+q \geq T: \qquad U_{ijtq} = 0 \tag{3.23}$$

$$\sum_{\substack{t \in \mathcal{T}_h \\ i \in \mathcal{N}_d}} H_{it} \geq \psi \tag{3.24}$$

Table 3.5: Definition of the equations in the logistics formulation

Equation	Name	Description
Equation 3.1	Objective Function	Maximize mission reward
Equations 3.2 - 3.7	Capacity Constraints	Enforce maximum propellant capacity and debris removal device capacity of the ADR Vehicle
Equations 3.8 - 3.11	Transformation Constraint	Define propellant expenditure over a transportation arc
Equations 3.12 - 3.19	Mass Balance Constraints	Define initial conditions and mass balance over the time-expanded network for the ADR Vehicle, propellant, and debris removal devices.
Equations 3.20 - 3.24	Operational Constraints	Define the behaviors of the ADR Vehicle and debris removal devices

CHAPTER 4

CASE STUDIES AND RESULTS

This section demonstrates several case studies utilizing the ADR mission optimization framework. To demonstrate the utility of the described method, three potential case studies are proposed, removing five, ten, and fifteen pieces of debris over one year, as well as one case study investigating multiple successive ADR missions. Each mission is described in Section 4.1, Section 4.2, Section 4.4, and Section 4.3, respectively. For each mission, the same set of debris described in Section 2.3 is used as considered debris for removal. The set of all considered debris is described in more detail in Appendix A. However, the individual mission parameters vary for the individual mission needs and are described in each section.

For each mission, the ADR Vehicle is given enough debris removal devices of each type to remove the maximum number of debris that are either all small or all large. This is done so that the optimizer may explore all possible subsets of debris that would satisfy the mission requirements. Note that by only equipping the ADR Vehicle with the debris removal devices that it will use, an even lower propellant expenditure may be computed. Additionally, the lowest time discretization that allows the optimizer to satisfy the minimum debris removals per year is used for each mission. Results with improved accuracy may be computed with a higher time discretization.

The mass of each small debris removal device is 175 kg, based on an ADR technical demonstration performed by Astroscale in 2021 [27]. The large debris removal devices shall have a mass of 100 kg each. This value was chosen based on conceptual studies performed by the Georgia Tech Research Institute to identify potential mission concepts for active debris removal [28].

For each scenario considered, the ADR Vehicle's dry mass and propellant capacity vary based on the payload size, which is the total mass of debris removal devices at the beginning of the mission. The structural mass is estimated using rocket sizing equations [29] with a payload ratio of 0.3 and a structural ratio of 0.2.

Each mission begins at an arbitrary start node, represented in the formulation presented in Section 3.5 as $\mathcal{N}_p$. The propellant and ΔV cost to go from this starting node to any debris is zero. It does not influence the optimization results or selected sequence or subset of debris for removal. This starting node only provides a starting location for the ADR Vehicle at the beginning of the mission. It is assumed that in an actual mission, the ADR Vehicle would begin at the first debris selected for removal after deployment by its launch vehicle.

4.1 Remove Five Pieces of Debris

4.1.1 Assumptions

This section presents the assumptions and input parameters associated with the ADR Vehicle, debris removal devices, considered debris, and timeline for a mission that attempts to remove five pieces of debris over one year. Five pieces of debris per year are chosen here since that is the minimum number of debris necessary to be removed in one year to stabilize the debris environment, as demonstrated by Liou et al. [4].

The following parameters are used in the mission optimization to determine the optimal subset and sequence of debris to remove during the mission. For this mission, the time-expanded network is formulated to have the largest discretization that will still allow the ADR Vehicle to remove five pieces of debris over the mission length of one year. Δt_t is set to allow the ADR Vehicle to travel over 68 days, and Δt_h is set to allow the ADR Vehicle five days for debris removal. These parameters produce a maximum number of five pieces of debris removals over one year. Given the number of time steps, considered debris, and allowable travel times, the trajectory optimization produced 15,400 possible transfers between nodes to consider.

4.1.2 Results

In the first case study evaluated, the most optimal path for the ADR Vehicle is found using the optimization framework. The solution presented is the solution that provides the maximum obtainable reward for the lowest cost in terms of propellant. This scenario will provide a reasonable baseline for the cost of a mission to eliminate the minimum amount of debris per year using high-thrust maneuvers.

A simplified path of the debris removal device is shown in Figure C.1. This figure summarizes the path that the ADR Vehicle takes to remove the optimal sequence of selected debris. The total calculated ΔV for this mission is 3.82 km/s, and the total propellant required is 9,531 kg. The estimated benefit obtained after one year by remediating this debris set is $358,430. Table 4.2 summarizes these results.

Figure 4.1 shows the removed debris' orbital elements, and Figure 4.2 shows the specific order taken from one debris to the next. The results show that the ADR Vehicle chose to first remove four large debris with similar orbits (in terms of semi-major axis, inclination, and RAAN) before taking an opportunity to travel to a high-reward group of small debris. Note that the optimization also considers other factors, such as the relative phasing of the debris at each time step and the optimal path over the entire time horizon, beyond the local vicinity of the orbital elements. Even though Small Debris Group 1 has a significantly different orbital plane from the other debris, its high reward made it a desirable target for removal. This set of results demonstrates the effectiveness of the system-level optimization framework. Full results are included in Appendix C.

Table 4.1: Mission parameters for removal of five pieces of debris

ADR Vehicle	
ADR Vehicle structural mass	3,000 kg
ADR Vehicle I_{sp}	316 s
Small debris removal device capacity	5
Large debris removal device capacity	5
Small Debris Removal Device	
Debris removal device mass	175 kg
Number deployed per removal	1
Large Debris Removal Device	
Debris removal device mass	100 kg
Number deployed per removal	1
Timeline	
Time for removal	5 days
Time for travel	68 days
Minimum debris removed per year	5
Total length of time step	73 days
Time of flight options	68 days

Table 4.2: Summary results of case study to remove five pieces of debris

Total number of debris removed	5
Total number of large debris removed	4
Total number of groups of small debris removed	1
Debris sequence	2, 6, 13, 11, 51
Total ΔV	3.82 km/s
Total propellant	9,531 kg
Total reward	$358,430

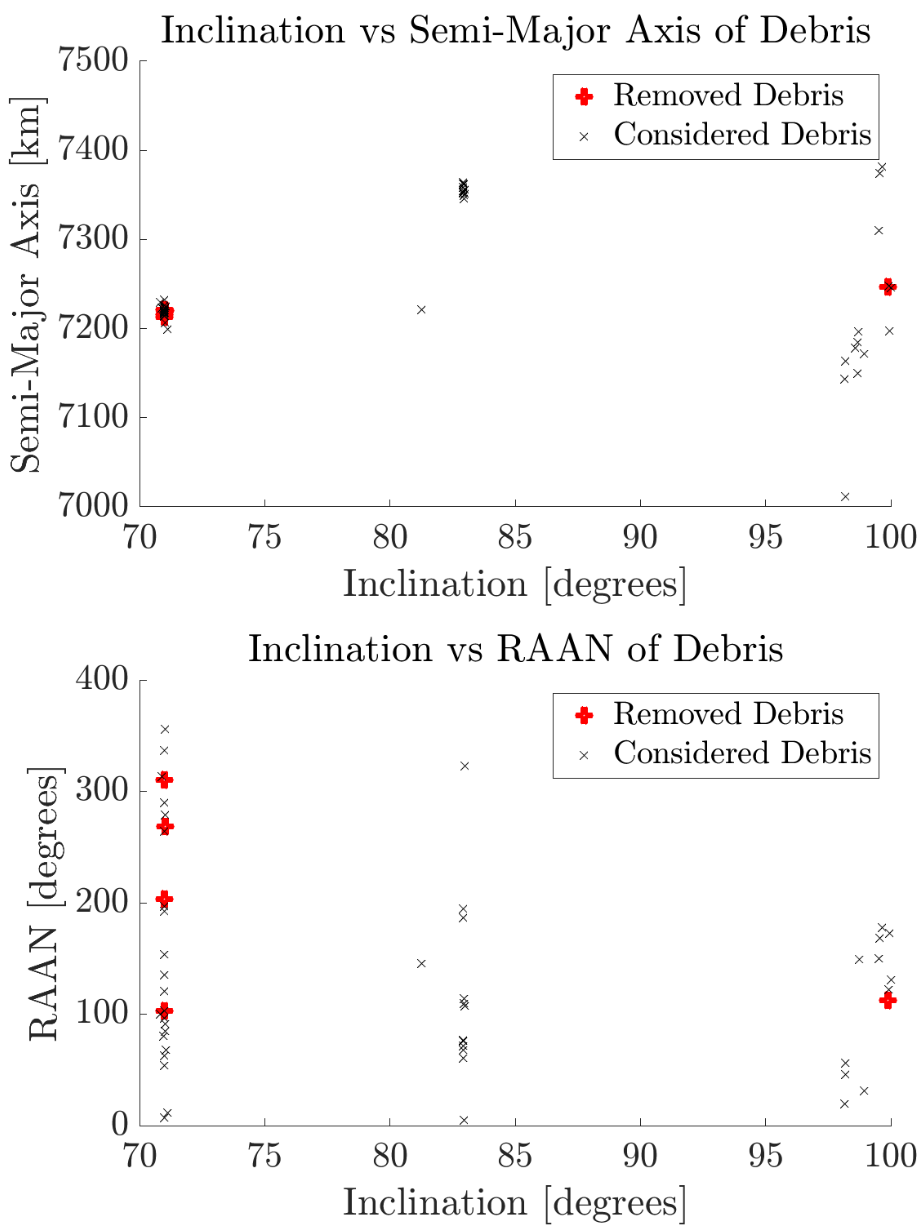

Figure 4.1: Orbital elements of five removed debris

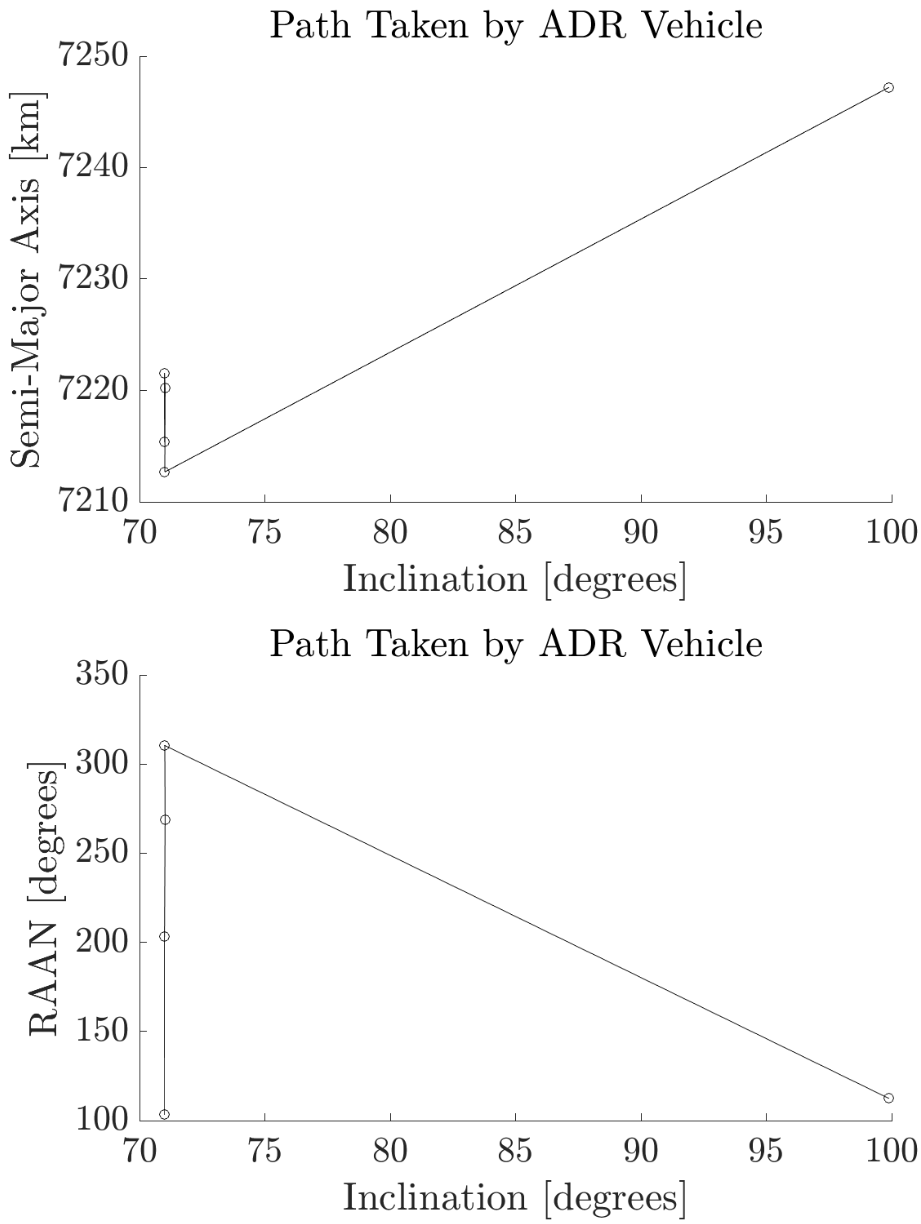

Figure 4.2: Path taken by ADR Vehicle over mission to remove five pieces of debris

4.2 Remove Ten Pieces of Debris

4.2.1 Assumptions

The parameters used for the mission design to remove ten pieces of debris are similar to those used in the prior case study, albeit with updated ADR Vehicle sizing and capacities for debris removal. The parameters defining the time-expanded network are similarly chosen to allow for a maximum number of ten pieces of debris removals in one year. The following parameters are used in the mission optimization to determine the optimal concept of operations for the mission to remove ten pieces of debris. The trajectory model for this scenario produced 33,880 transfers between nodes to consider.

4.2.2 Results

The most optimal mission for the ADR Vehicle is similarly computed using the optimization framework. Figure D.1 shows the path of the ADR Vehicle over the time-expanded network. Although the most optimal path for removal consisted of a different sequence of debris from the results presented in Section 4.1.2, the optimizer still chose to remove a set of large debris with high rewards before removing the most high-reward group of small debris.

The total calculated ΔV for this mission was 3.99 km/s, and the total propellant required is 20,346 kg. This larger required propellant compared to the propellant required in the last case study above is primarily due to the larger payload and structural mass necessary to accommodate a larger mission, as well as the larger ΔV associated with more maneuvers between debris. The estimated benefit obtained after one year by remediating this set of debris is $708,430. More detail about these specific results is included in Appendix D.

Table 4.3: Mission parameters for removal of ten pieces of debris

ADR Vehicle	
ADR Vehicle structural mass	6,000 kg
ADR Vehicle I_{sp}	316 s
Small debris removal device capacity	10
Large debris removal device capacity	10
Small Debris Removal Device	
Debris removal device mass	175 kg
Number deployed per removal	1
Large Debris Removal Device	
Debris removal device mass	100 kg
Number deployed per removal	1
Timeline	
Time for removal	5 days
Time for travel	31 days
Minimum debris removed per year	10
Total length of time step	36 days
Time of flight options	31 days

Table 4.4: Summary results of case study to remove ten pieces of debris

Total number of debris removed	10
Total number of large debris removed	9
Total number of groups of small debris removed	1
Debris sequence	32, 1, 17, 31, 6, 10, 46, 12, 19, 51
Total ΔV	3.99 km/s
Total propellant	20,346 kg
Total reward	$708,430

Table 4.5: Summary results of case studies considering removal of five and ten pieces of debris

Debris Removed	**Reward** [USD]	**Percent Increase** [%]	**Required Propellant** [kg]	**Percent Increase** [%]	**Required ΔV** [km/s]	**Percent Increase** [%]
5	358,430	-	9,531	-	3.82	-
10	708,430	97.65	20,346	113.47	3.99	4.45

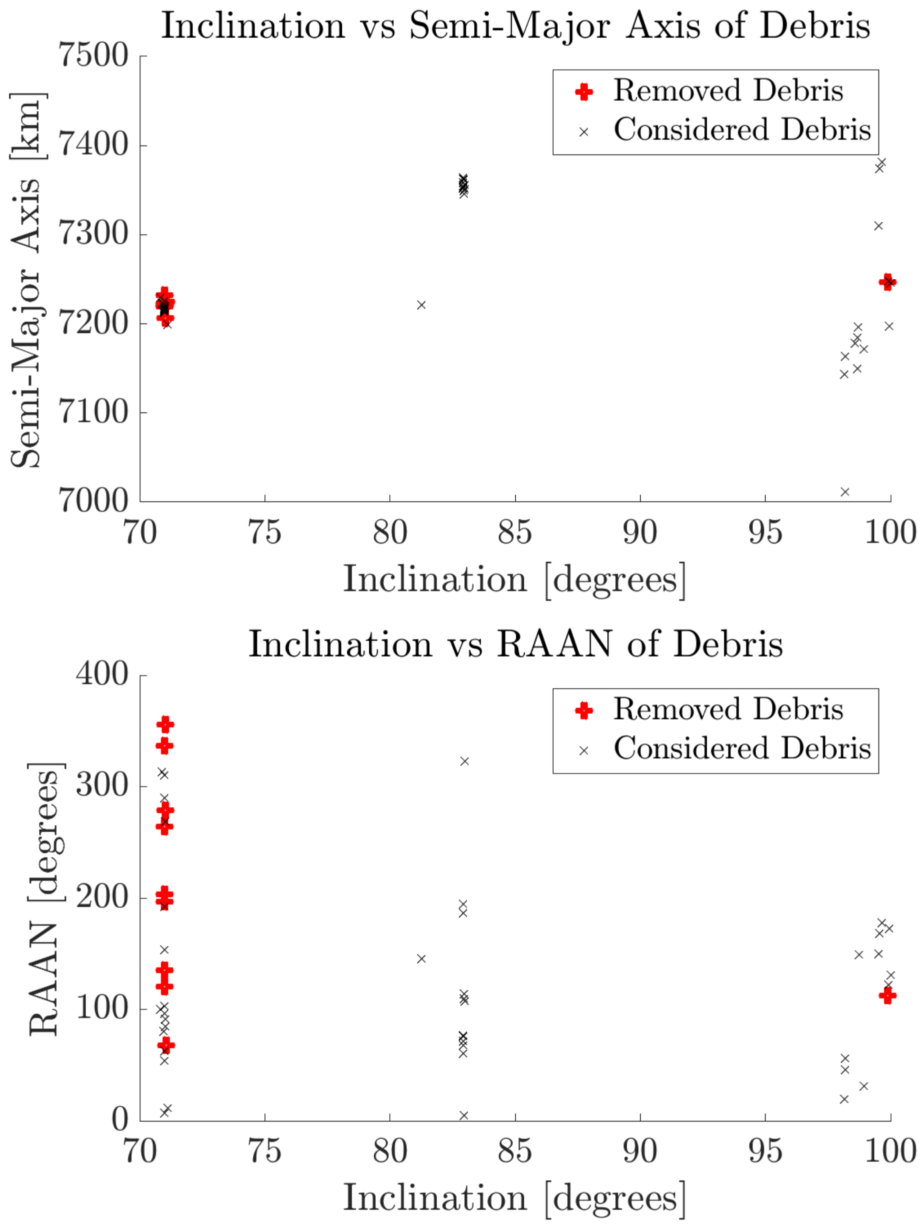

Figure 4.3: Orbital elements of ten removed debris

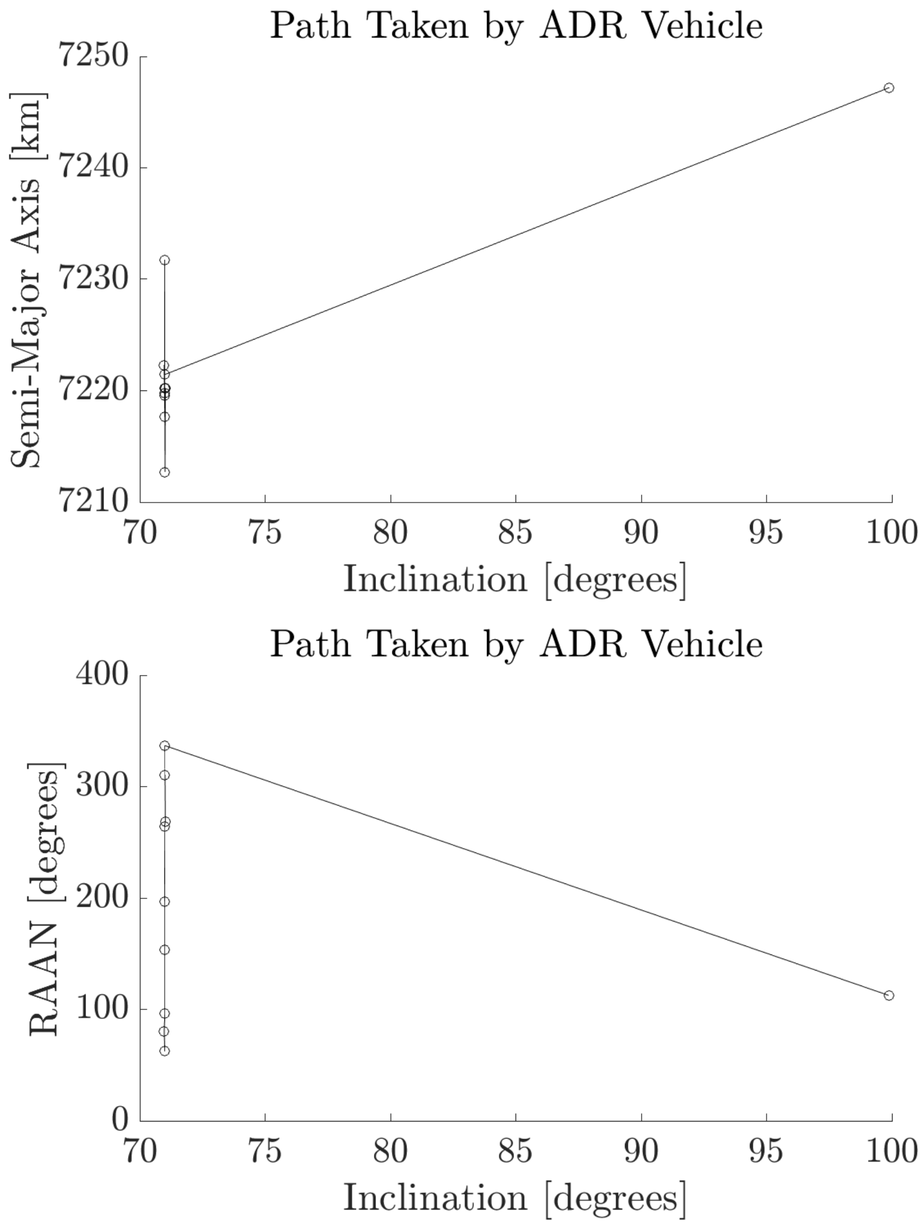

Figure 4.4: Path taken by ADR Vehicle over mission to remove ten pieces of debris

4.3 Remove Five Pieces of Debris: Subsequent Launch

4.3.1 Assumptions

This case study investigates the feasibility of several subsequent ADR missions. A second mission to remove five pieces of debris as a follow-up to the mission presented in Section 4.1 is investigated. For this mission, it is assumed that the beginning of the mission is one year after the beginning of the mission described in Section 4.1. Since this mission occurs after the prior mission to remove five pieces of debris, the five pieces of debris that were selected for removal in Section 4.1.2 are omitted from the data set of debris to consider. However, the structural mass, debris removal device capacity, desired number of debris for removal, and parameters for the time-expanded network remain the same as the prior mission. Other than the considered debris set, the start parameters for the second mission are independent of those of the first.

4.3.2 Results

The optimization produced a mission sequence that required significantly less propellant and ΔV to obtain the maximum reward. Since this data set omitted the group of small debris that produced the greatest reward, there were no groups of small debris that exceeded the reward of any individual large debris. Many of the large debris considered are in extremely similar orbital planes, and do not require expensive maneuvers to transfer between them. For this reason, the proposed follow-up mission does not require as much ΔV or propellant to obtain the maximum obtainable reward.

The total ΔV to remove ten pieces of debris over two missions was 3.89 km/s, while the total ΔV to remove ten pieces of debris over one single mission was 3.99 km/s. Sending two smaller ADR Vehicles produces a mission that obtains the same cumulative reward over two years as one larger mission to remove ten pieces of debris for a significantly lower amount of propellant, requiring approximately 10,521 kg less propellant. These results suggest that it may be more practical to have multiple subsequent ADR missions to remove more numerous amounts of space debris, if the goal is to target both small and large space debris.

Table 4.6: Mission parameters for subsequent removal of five pieces of debris

ADR Vehicle	
ADR Vehicle structural mass	6,000 kg
ADR Vehicle I_{sp}	316 s
Propellant capacity	9,531
Small debris removal device capacity	5
Large debris removal device capacity	5
Small Debris Removal Device	
Debris removal device mass	175 kg
Number deployed per removal	1
Large Debris Removal Device	
Debris removal device mass	100 kg
Number deployed per removal	1
Timeline	
Time for removal	5 days
Time for travel	68 days
Minimum debris removed per year	5
Total length of time step	73 days
Time of flight options	68 days

Table 4.7: Summary results of subsequent case study to remove five pieces of debris

Total number of debris removed	5
Total number of large debris removed	5
Total number of groups of small debris removed	0
Debris sequence	31, 10, 46, 12, 19
Total ΔV	0.07 km/s
Total propellant	294 kg
Total reward	$350,000

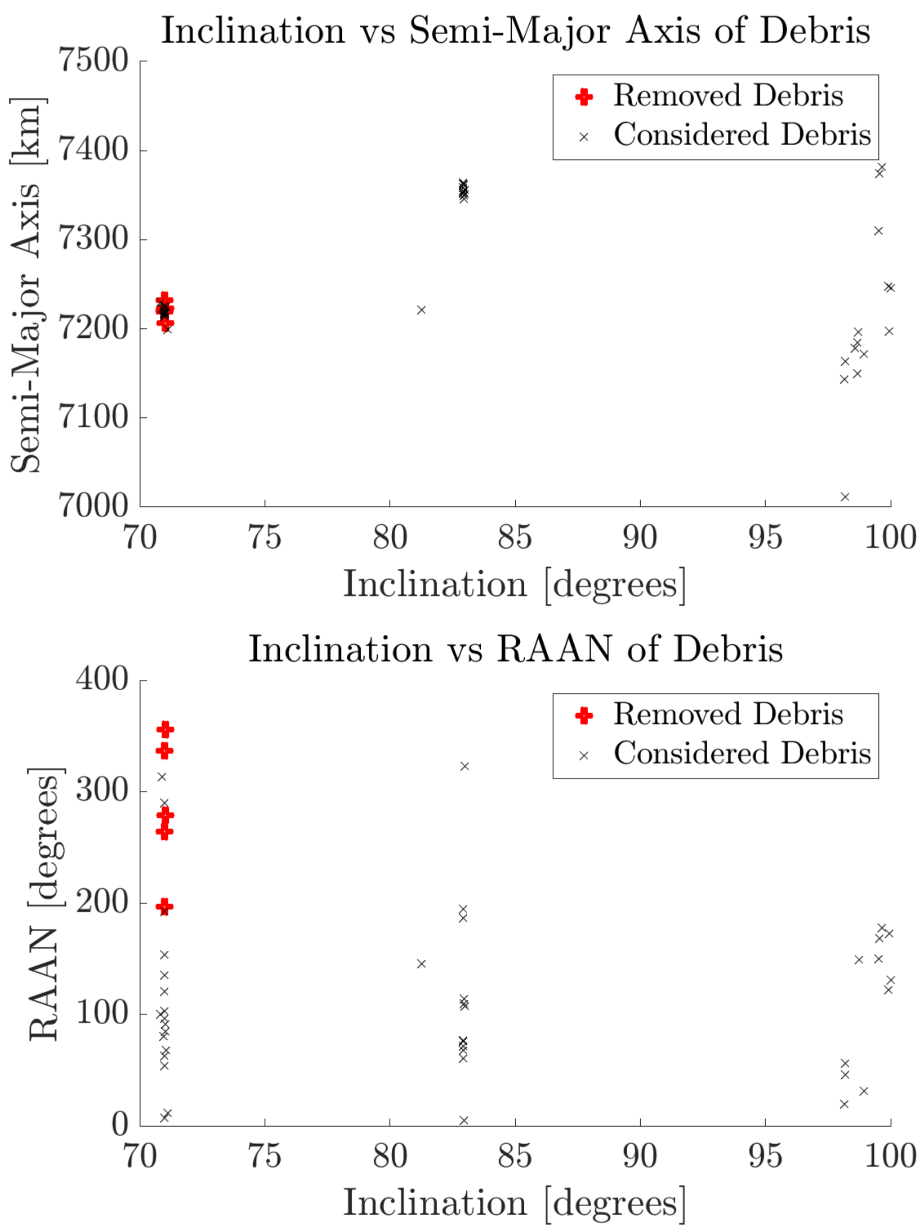

Figure 4.5: Orbital elements of five removed debris in subsequent launch

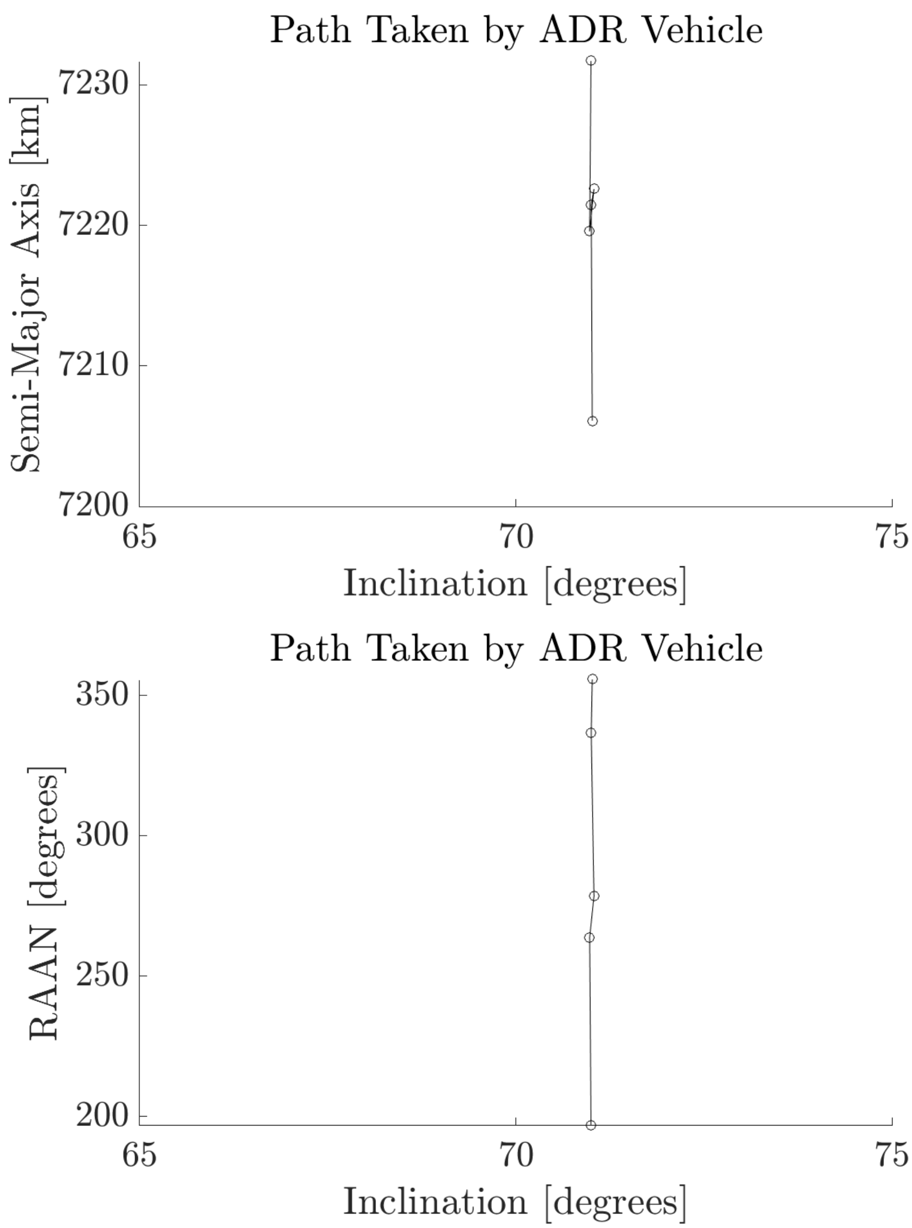

Figure 4.6: Path taken by ADR Vehicle over subsequent launch to remove five pieces of debris

4.4 Remove Fifteen Pieces of Debris

4.4.1 Assumptions

To demonstrate the flexibility of the proposed framework, an alternate approach is examined to remove fifteen pieces of debris. If the objective of the optimization framework is always to obtain the maximum possible reward for debris removal, the required ΔV and propellant to remove the most high-reward set of debris increases very quickly as the number of desired debris removed increases. Removing the most high-reward set of debris is realistically infeasible for a mission to remove fifteen or more pieces of debris with the given set of considered debris for removal, as the ΔV and propellant required increases past what is reasonable for one launch.

The optimization framework also allows a user to determine the maximum potential reward within a set of mission constraints. The same set of considered debris is used for the presented case study as in the prior two case studies. The size of the ADR Vehicle and debris removal device capacity are similarly updated. However, instead of attempting to obtain the maximum-reward subset of debris from the entire set of debris with initial constraint on propellant, the optimization framework is tasked with determining the maximum reward possible with some propellant constraint. This way, given some maximum allowable ADR Vehicle propellant capacity, a mission CONOPS may be designed that maximizes reward within those constraints.

The propellant provided to the ADR Vehicle at the beginning of the mission is 22,500 kg. This propellant capacity is congruent with the same structural, propellant, and payload ratios set for the prior case studies. Additionally, the ADR Vehicle is given a debris removal device capacity of 15 small debris removal devices and 15 large debris removal devices. The ADR Vehicle is also given additional time of flight options for this case study, being permitted to stay at a debris node for an additional time step if no optimal path to the next node currently exists. The trajectory optimization for this scenario produced 98,560 possible transfers between nodes to consider.

4.4.2 Results

Although this mission does not obtain the maximum potential reward from debris removal like in Section 4.1.2 and Section 4.2.2 and does not succeed in removing any small debris groups, the mission still obtains the maximum reward within the given mission constraints and ADR Vehicle capacity. By only removing large debris in similar orbits, the ADR Vehicle can still remove fifteen pieces of debris in one mission and obtain a significant reward. However, for a presented mission of this size, combining the removal of large debris and small debris groups into one mission is likely infeasible.

This mission's total calculated ΔV is 0.93 km/s, and the total propellant required is 8,979 kg. The ΔV required for this mission is considerably lower than the ΔV required for the missions presented in Sections 4.1 and 4.2. This is because in this mission, the ADR Vehicle is not required to obtain the maximum reward by removing the most high-reward group of small debris, which saved the ADR Vehicle from completing an expensive maneuver to change its orbital plane significantly. Even though the reward from this mission is $8,430 less than the total obtainable reward, the presented framework still produced a feasible mission that targets many pieces of debris in one mission. The ΔV required for this mission is significantly less than the ΔV required for the missions to remove the highest-reward sets of five and ten pieces of debris seen in the prior two case studies. However, there is still a considerable amount of required propellant. This is due to the increased structural and payload mass of the ADR Vehicle to accommodate the removal of fifteen pieces of debris in one mission.

Table 4.8: Mission parameters for removal of fifteen pieces of debris

ADR Vehicle	
ADR Vehicle structural mass	9,000 kg
ADR Vehicle I_{sp}	316 s
Propellant capacity	22,500 kg
Small debris removal device capacity	15
Large debris removal device capacity	15
Small Debris Removal Device	
Debris removal device mass	175 kg
Number deployed per removal	1
Large Debris Removal Device	
Debris removal device mass	100 kg
Number deployed per removal	1
Timeline	
Time for removal	5 days
Time for travel	19 days
Minimum debris removed per year	15
Total length of time step	24 days
Time of flight options	19, 43 days

Table 4.9: Summary results of case study to remove fifteen pieces of debris

Total number of debris removed	15
Total number of large debris removed	15
Total number of groups of small debris removed	0
Debris sequence	5, 32, 3, 8, 9, 25, 16, 2, 29, 1, 17, 33, 18, 31, 6
Total ΔV	0.93 km/s
Total propellant	8,979 kg
Total reward	$1,050,000

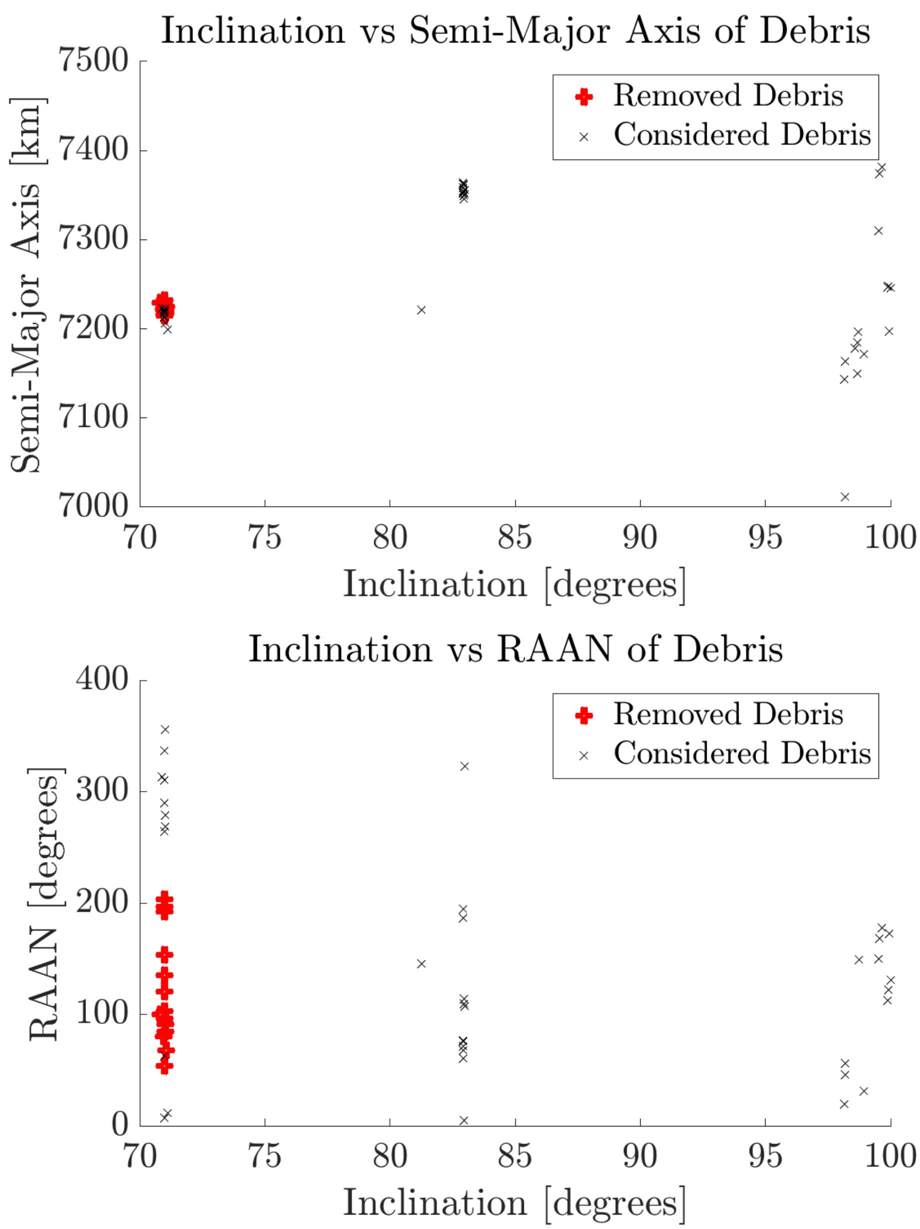

Figure 4.7: Orbital elements of fifteen removed debris

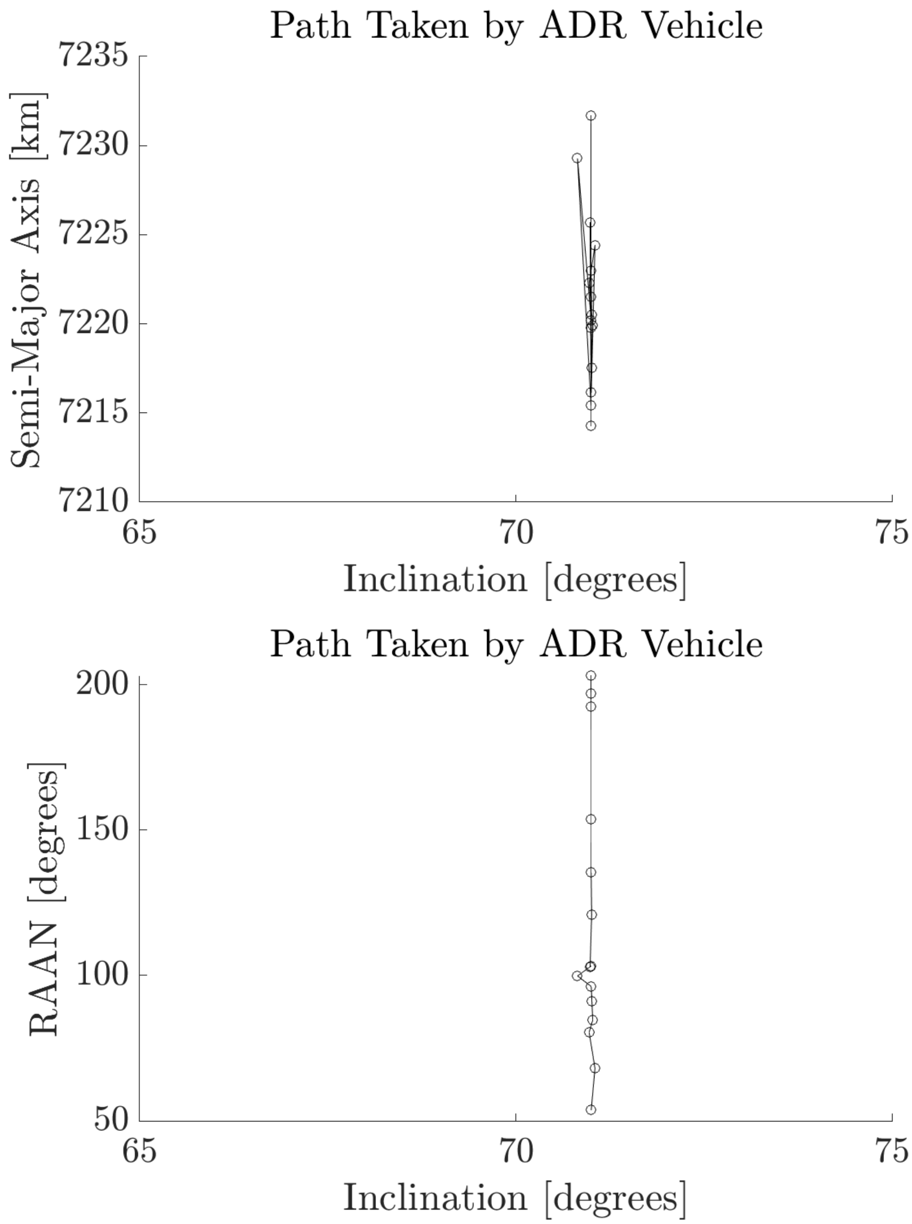

Figure 4.8: Path taken by ADR Vehicle over mission to remove fifteen pieces of debris

4.5 Main Findings

The case studies presented above demonstrate the high-level concept of operations for several missions to remediate and address the space debris problem. The presented optimal mission solutions led to several notable findings.

First, the most optimal number of debris to consider for removal in one mission for this framework is likely to be around five pieces of debris. The difference in ΔV between the results presented for removing five and ten pieces of debris is only 0.2 km/s. However, the difference in reward is \$350,000, which is a 98% increase. Nonetheless, the required propellant for a mission to remove ten pieces of debris is 10,521 kg more than the required propellant for a mission to remove five pieces of debris, which is a 113% increase. This increased propellant is due to the increased structural and payload mass required to accommodate a mission of this size. These results suggest that if the mission objective is to maximize reward from debris removal by combining large and small debris removal into one mission, the ideal number of debris to remove in a given mission is probably less than ten pieces of debris. Additionally, the results from Section 4.3 demonstrated that having two missions to remove debris is less expensive while producing an identical reward. Removing more than ten to fifteen pieces of debris in one single mission over one year by one ADR Vehicle will likely be infeasible.

Even though the presented case study to remove fifteen pieces of debris did not address small debris, it still obtained the most significant reward to required propellant ratio, as seen in Table 4.10. Two missions removing five pieces of debris each produced a large reward to required propellant ratio as well, suggesting that missions to remove both large and small debris may be split into multiple launches and ADR Vehicles. These reward to required propellant ratios provide insight into how many pieces of debris per year should realistically be removed in a single mission that addresses both large and small debris.

Debris Removed	**Reward** [USD]	**Required Propellant** [kg]	**Reward to Required Propellant Ratio**
5	358,430	9,531	36.61
10	708,430	20,346	34.62
15	1,050,000	8,979	116.94
10, Two missions	708,430	9,825	72.10

Table 4.10: Reward versus required propellant ratios for each considered case study

Grouping many pieces of small debris unevenly increased the mission's reward. Suppose all small pieces of debris had a more even distribution across small debris groups. In that case, any individual group may not have exceeded the value of the most rewarding large debris, and the optimizer may not have been incentivized to select them for removal. However, since there was one very large group of small debris with a high reward, the optimizer selected it for removal and was able to increase its reward. Small debris was grouped agnostically with respect to the considered large debris. There may be alternate groupings of small debris that are closer in orbit to the other large debris chosen for removal that may produce results using the same framework requiring even lower ΔV and propellant.

Additionally, it was initially undetermined if the mass of each debris removal device would affect the selected order of debris to remove. Hypothetically, the optimizer may choose to remove a group of small debris first so that it may release the larger mass of the small debris removal device earlier in the mission and have subsequent maneuvers that require less propellant due to the ADR Vehicle's decreased mass. However, the results presented here show that, at least for the considered parameters and debris set, the difference in mass between debris removal device types is negligible, and the order of debris to remove is much more significant to the results.

It should be noted that for the presented case studies in Section 4.1, Section 4.3, and Section 4.2, the optimization framework was tasked with finding a mission that would obtain the maximum possible reward given the set of considered debris and input parameters. However, Section 4.4 demonstrated how one of the benefits of this framework is that it is highly flexible. It is possible to consider alternate missions with smaller or larger ADR Vehicles capable of removing more or less debris than the results presented here. The results here should be interpreted as high-level concepts of operation demonstrating the feasibility of ADR missions.

CHAPTER 5

CONCLUSION

This method introduces an optimization framework to determine the most optimal concept of operations for an ADR mission targeting multiple types of debris in a single mission. First, a grid search and a high-fidelity trajectory model generate a graph of maneuver costs for all debris throughout the time-expanded network. Next, a model representing the ADR mission logistics is formulated as a MILP and iteratively optimized using a binary search. Given the model's complexity and the requirements of an ADR mission, a time-expanded network is a practical approach to solving this problem. The presented framework successfully obtains the lowest-ΔV mission that still achieves the highest possible reward from debris removal.

Formulating the logistics of the ADR mission as a time-expanded network removes time from the list of decision variables. This simplifies the MILP while maintaining a realistic model of the mission's logistics. The formulation presented here is highly generalizable and flexible and can optimize a range of potential ADR missions to combat the space debris problem. This framework should be used as a mission design tool to size and estimate potential future ADR missions. Its flexibility provides a realistic benchmark for an optimal mission to remove several types of space debris.

Several case studies test this approach. The case studies demonstrate the feasibility of a proposed ADR mission and the value of the presented optimization framework. Significantly, this framework produced several key findings. For the considered debris set used in this thesis, the ΔV and propellant required to perform the mission increase past probable feasibility after a certain number of debris removals per mission. A mission seeking to remove more than this amount of debris should be broken into multiple missions or decrease the maximum desired reward from debris removals. Nonetheless, some missions that address both large and small debris were found to be feasible.

Additionally, grouping small debris strategically provided an added reward to the mission while maintaining mission feasibility. Having one very large group of small debris that can all be removed by one deployed small debris removal device provided the ADR Vehicle the opportunity to combat multiple types of dangerous space debris in one mission and increase its potential reward. Addressing multiple types of space debris aligns with recommended space debris mitigation strategies [6].

Lastly, the mass of the debris removal device had a negligible effect on the optimization results for each case study. Additional scenarios should be investigated with a more significant mass difference between debris removal device types to determine if and when this mass difference affects the mission solution.

Ultimately, this tool should be used to evaluate mission concepts that address the most pressing dangers posed by space debris. Both small and large debris pose catastrophic effects to the orbital environment. For this reason, both of these types of debris need to be addressed through ADR missions. The optimization framework shown here demonstrates that addressing both types of debris together is feasible and may also provide an increased reward.

Appendices

APPENDIX A
SUMMARY OF DEBRIS CONSIDERED

The full set of large and small debris considered for removal in each optimization is presented below. Debris 1 through 50 are large pieces of debris, while debris 51 through 55 are small debris groupings. The orbital elements presented for each small debris grouping serve as representative models for the entire debris group.

Table A.1: All debris considered in debris set

Name	**Index**	**Reward** [USD]	**Mass** [kg]	**Semi-Major Axis** [km]	**Eccen-tricity**	**Incli-nation** [degrees]	**Argu-ment of Perigee** [degrees]	**RAAN** [degrees]
SL-16 R/B - 22,566	1	70,000	9,000	7,220.5	0.001	71.01	81.42	120.84
SL-16 R/B - 22,220	2	70,000	9,000	7,215.4	0.001	71.00	226.29	103.21
SL-16 R/B - 31,793	3	70,000	9,000	7,222.3	0.000	70.97	262.61	80.43
SL-16 R/B - 26,070	4	70,000	9,000	7,218.8	0.002	71.00	298.15	7.31
SL-16 R/B - 16,182	5	70,000	9,000	7,216.1	0.001	71.00	2.17	53.76
SL-16 R/B - 20,625	6	70,000	9,000	7,221.5	0.001	71.00	55.19	203.31
SL-16 R/B - 27,006	7	70,000	9,000	7,374.2	0.001	99.55	244.85	167.82
SL-16 R/B - 23,705	8	70,000	9,000	7,219.9	0.001	71.02	247.51	84.66
SL-16 R/B - 25,407	9	70,000	9,000	7,217.6	0.001	71.01	168.52	91.16
SL-16 R/B - 23,405	10	70,000	9,000	7,219.6	0.001	70.98	275.18	263.78
SL-16 R/B - 17,974	11	70,000	9,000	7,212.7	0.002	71.01	325.59	310.39
SL-16 R/B - 23,088	12	70,000	9,000	7,221.5	0.000	71.00	5.21	336.78
SL-16 R/B - 22,285	13	70,000	9,000	7,220.2	0.000	71.02	50.75	268.57
SL-16 R/B - 22,803	14	70,000	9,000	7,214.2	0.002	70.99	326.35	289.55
SL-16 R/B - 19,650	15	70,000	9,000	7,217.7	0.001	71.00	138.76	62.75
SL-16 R/B - 24,298	16	70,000	9,000	7,229.3	0.002	70.82	201.66	99.85

SL-16 R/B - 28,353	17	70,000	9,000	7,223.0	0.000	71.00	184.44	135.39
SL-16 R/B - 17,590	18	70,000	9,000	7,214.3	0.001	71.00	253.95	192.39
SL-16 R/B - 19,120	19	70,000	9,000	7,206.1	0.002	71.02	121.53	355.80
SL-16 R/B - 25,400	20	70,000	9,000	7,185.0	0.001	98.66	51.64	329.12
ENVISAT - 27,386	21	70,000	7,800	7,143.0	0.000	98.17	87.73	19.17
METEOR 3 M - 27,001	22	70,000	2,500	7,381.8	0.001	99.65	328.95	178.01
ADEOS - 24,277	23	70,000	3,560	7,171.6	0.000	98.93	86.93	30.94
H-2A R/B - 27,601	24	70,000	3,000	7,163.1	0.007	98.18	310.35	45.96
SL-12 R/B(2) - 15,334	25	70,000	2,440	7,220.2	0.001	71.00	263.88	96.21
CZ-2D R/B - 37,932	26	70,000	4,000	7,196.4	0.004	98.71	187.96	329.51
SL-8 R/B - 10,732	27	70,000	1,435	7,358.5	0.002	82.93	207.01	76.70
H-2 R/B - 24,279	28	70,000	2,700	7,460.7	0.030	98.76	300.77	149.03
COSMOS 2322 - 23,704	29	70,000	3,250	7,225.7	0.001	70.99	45.19	102.86
SL-8 R/B - 21,090	30	70,000	1,435	7,354.8	0.002	82.92	356.57	60.51
COSMOS 2406 - 28,352	31	70,000	3,250	7,231.7	0.001	71.00	69.63	197.03
COSMOS 2278 - 23,087	32	70,000	3,250	7,224.4	0.001	71.05	170.10	68.05
COSMOS 1943 - 19,119	33	70,000	3,250	7,219.8	0.001	71.00	356.12	153.80
ADEOS 2 - 27,597	34	70,000	3,680	7,178.1	0.000	98.59	70.32	337.57
SL-16 R/B - 25,861	35	70,000	9,000	7,011.5	0.002	98.19	55.79	56.19
SL-12 R/B(2) - 15,772	36	70,000	2,440	7,199.0	0.004	71.11	294.90	11.29
SL-8 R/B - 10,693	37	70,000	1,435	7,351.1	0.002	82.99	358.17	322.73
COSMOS 1844 - 17,973	38	70,000	3,250	7,223.4	0.003	70.90	113.22	313.08
ARIANE 5 R/B - 27,387	39	70,000	2,575	7,149.7	0.003	98.69	162.52	358.25
SL-8 R/B - 7,594	40	70,000	1,435	7,345.8	0.001	82.95	294.25	109.27
SL-8 R/B - 23,180	41	70,000	1,435	7,349.0	0.003	82.95	165.45	113.97
SL-8 R/B - 10,138	42	70,000	1,435	7,363.7	0.002	82.94	10.37	75.70
SL-8 R/B - 13,917	43	70,000	1,435	7,353.1	0.003	82.94	200.13	71.59
SL-3 R/B - 13,719	44	70,000	1,100	7,221.5	0.007	81.26	213.24	145.45
SL-8 R/B - 14,625	45	70,000	1,435	7,362.0	0.002	82.93	62.13	194.22
COSMOS 2082 - 20,624	46	70,000	3,250	7,222.6	0.002	71.04	323.04	278.57
SL-8 R/B - 12,092	47	70,000	1,435	7,352.6	0.003	82.94	57.58	68.11
SL-8 R/B - 9,044	48	70,000	1,435	7,355.4	0.001	82.99	234.95	107.35
COSMOS 1275 - 12,504	49	70,000	800	7,362.1	0.004	82.96	315.37	4.99

SL-8 R/B - 16,292	50	70,000	1,435	7,352.6	0.003	82.93	43.26	186.40
Small Debris Group 1	51	78,430	-	7,247.2	0.012	99.90	7.62	112.40
Small Debris Group 2	52	50,370	-	7,247.6	0.002	99.90	15.38	122.10
Small Debris Group 3	53	42,780	-	7,245.9	0.003	100.03	345.99	130.93
Small Debris Group 4	54	33,580	-	7,196.9	0.007	99.96	311.00	172.77
Small Debris Group 5	55	28,750	-	7,309.9	0.009	99.53	318.78	149.88

APPENDIX B

ORBIT VIZUALIZATIONS OF DIFFERENT SETS OF DEBRIS

This appendix provides a simplified visualization of the orbits of different subsets of debris considered from each section. Figure B.1 shows the orbits of the fifty considered large pieces of debris. Figure B.2 shows the representative orbits of each small debris group. Figure B.3, Figure B.4, Figure B.5, and Figure B.6 show the orbits of the debris collected in the case studies described in Sections 4.1, 4.2, 4.3, and 4.4, respectively.

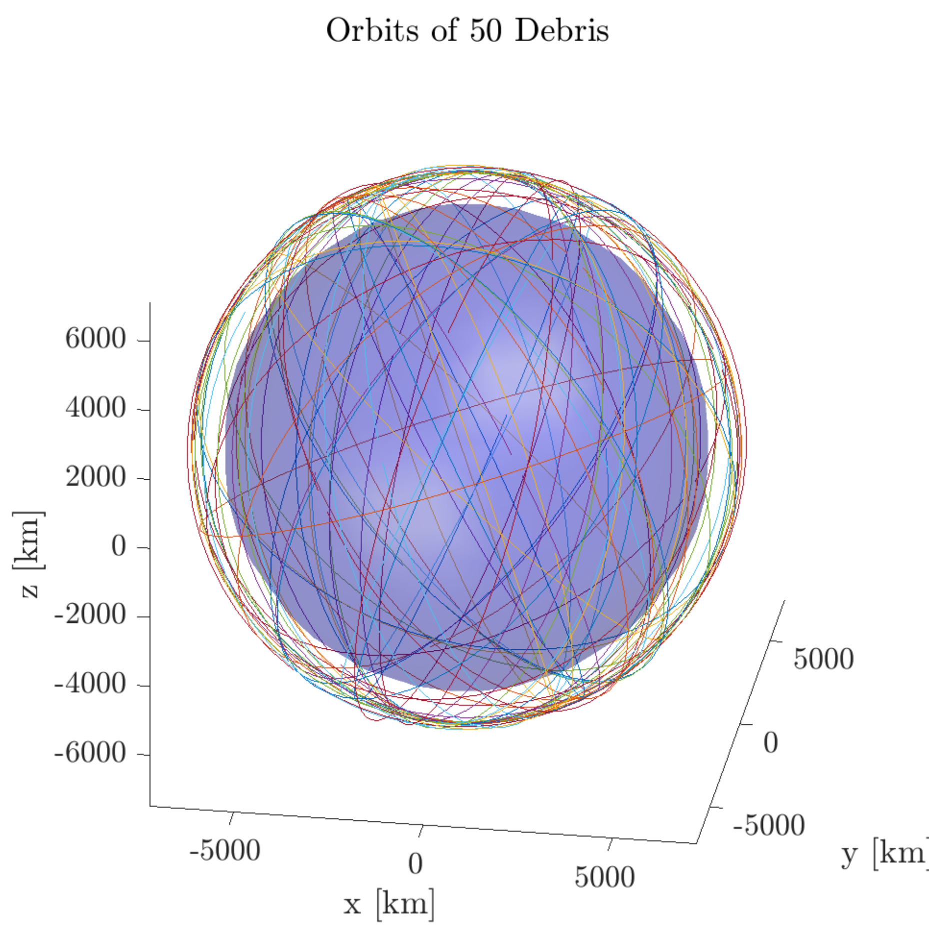

Figure B.1: Orbits of considered large debris

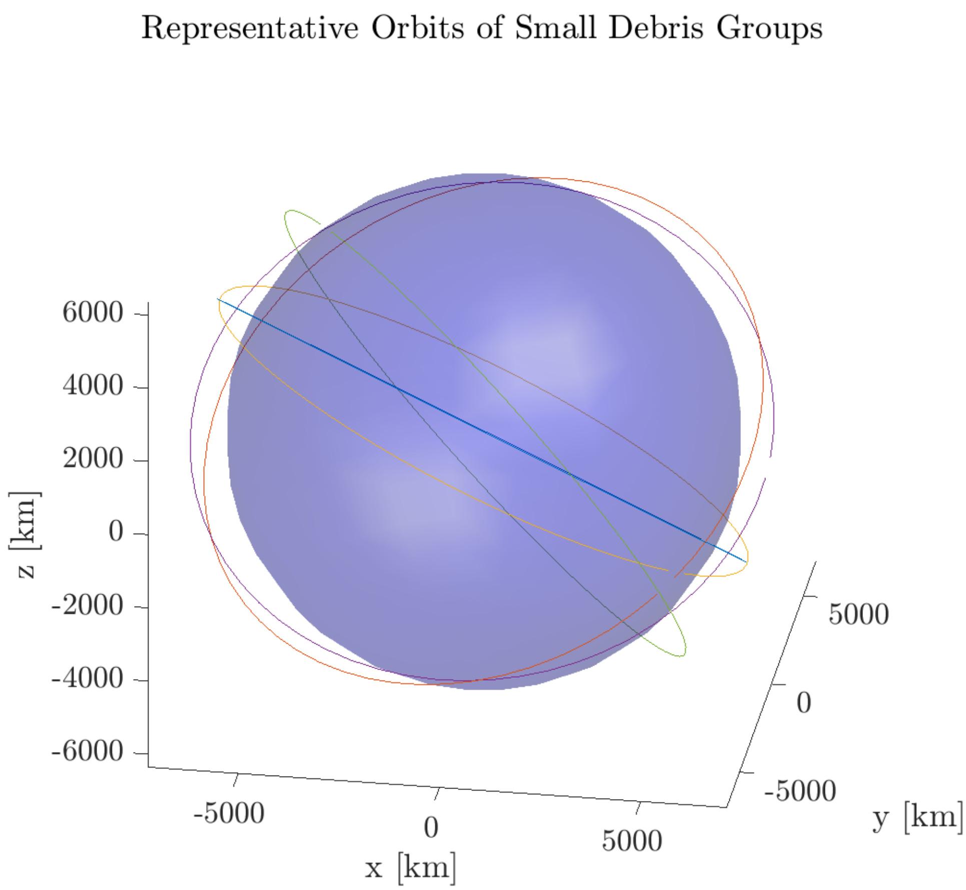

Figure B.2: Representative orbits of small debris groups

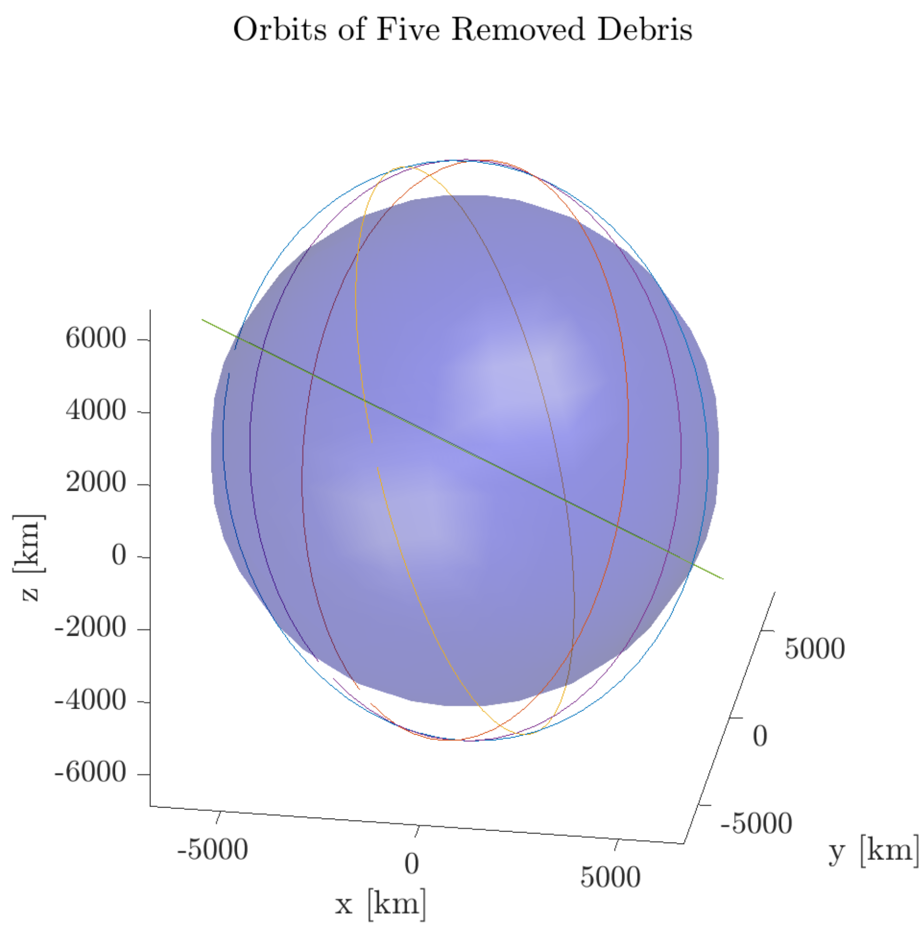

Figure B.3: Orbits of five removed debris

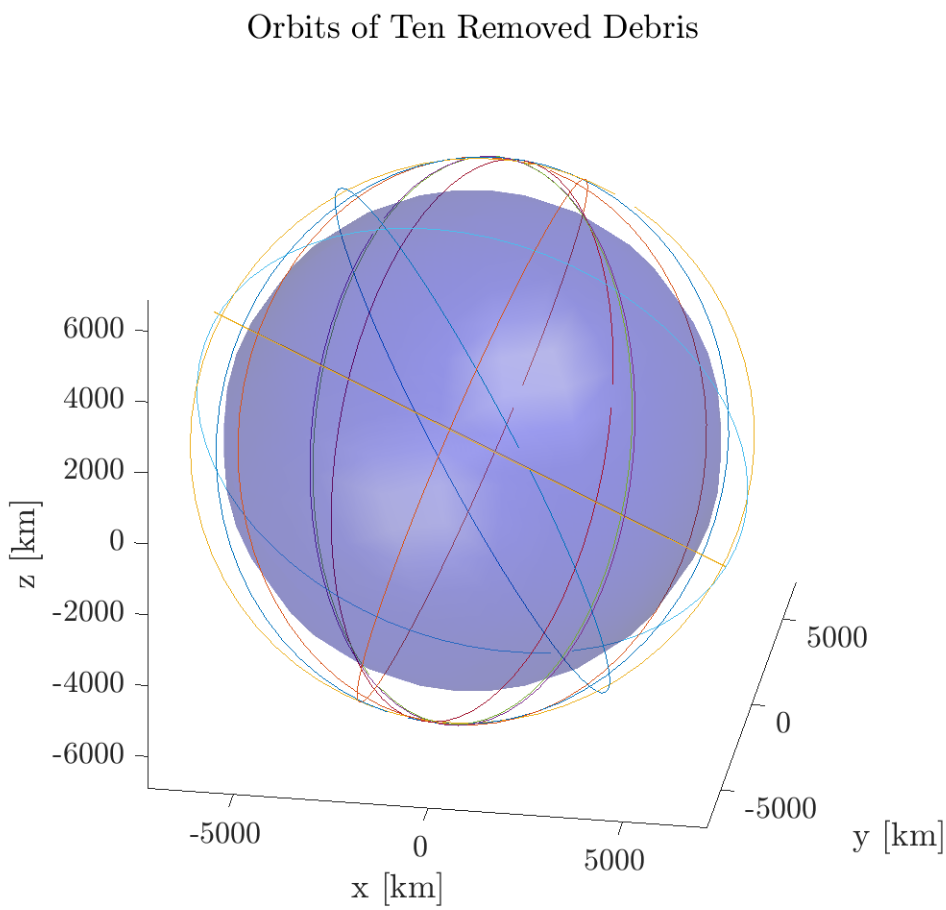

Figure B.4: Orbits of ten removed debris

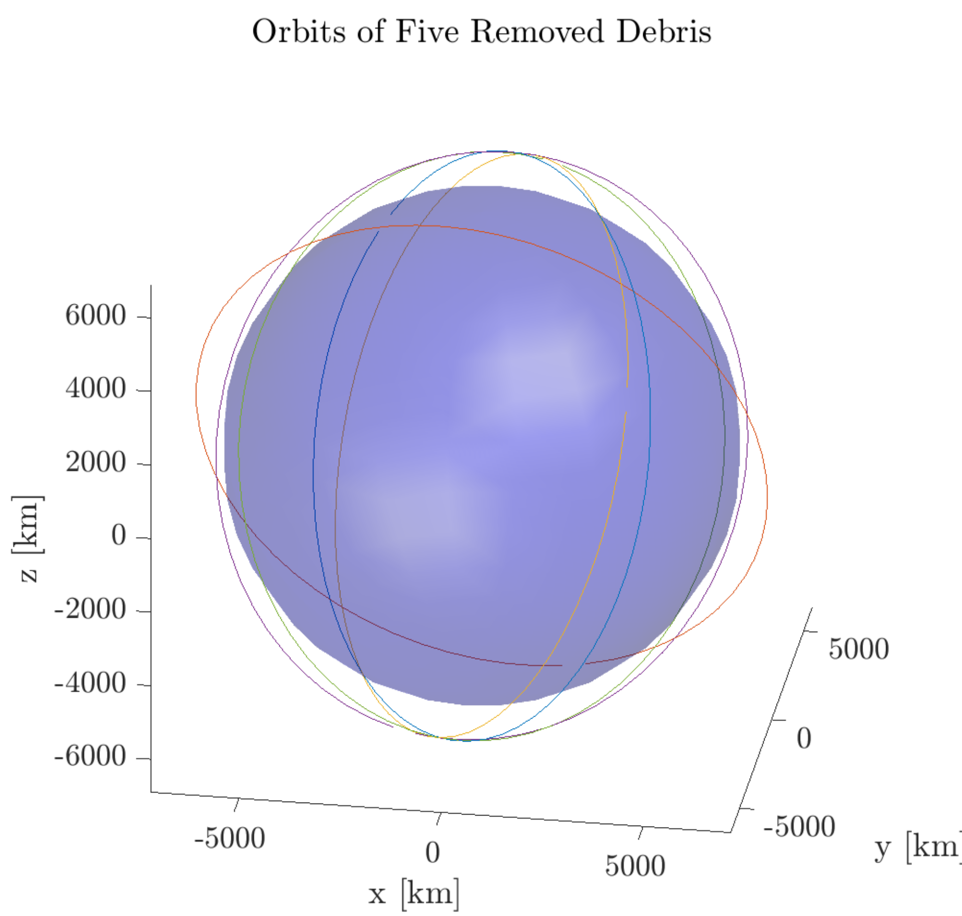

Figure B.5: Orbits of five removed debris in subsequent launch

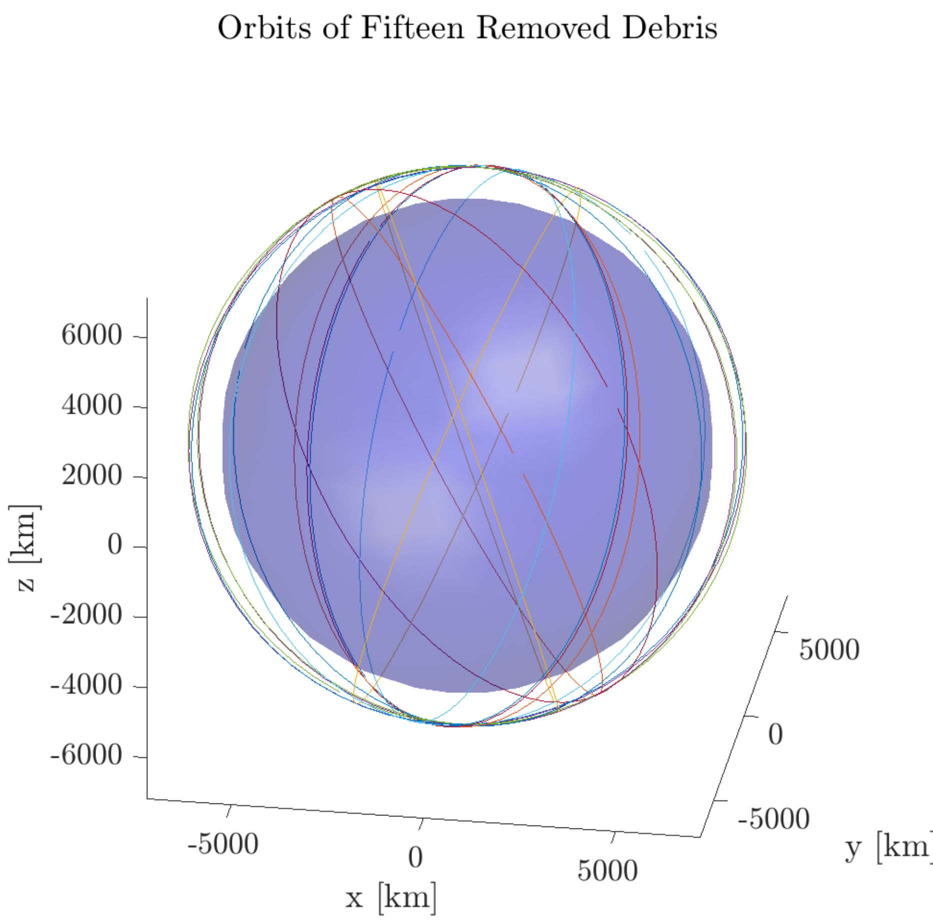

Figure B.6: Orbits of fifteen removed debris

APPENDIX C

FULL RESULTS: REMOVE FIVE PIECES OF DEBRIS

This appendix includes further details about the results from the case study presented in Section 4.1, including the full timeline and allocation of variables and resources over the duration of the mission.

Table C.1: Full timeline of mission to remove five pieces of debris

Time Step	**Debris Node**	**Remaining propellant** [kg]	**ΔV** [km/s]	**Remaining Small Debris Removal Devices**	**Remaining Large Debris Removal Devices**	**Total Reward** [USD]
0	Start	9,531		5	5	0
5	Start	9,531		5	5	0
73	2	9,531		5	5	0
78	2	9,531		5	4	70,000
146	6	9,444	0.020	5	4	70,000
151	6	9,444		5	3	140,000
219	13	9,386	0.013	5	3	140,000
224	13	9,386		5	2	210,000
292	11	9,254	0.031	5	2	210,000
297	11	9,254		5	1	280,000
365	51	0	3.76	4	1	280,000
370	51	0		4	1	358,430

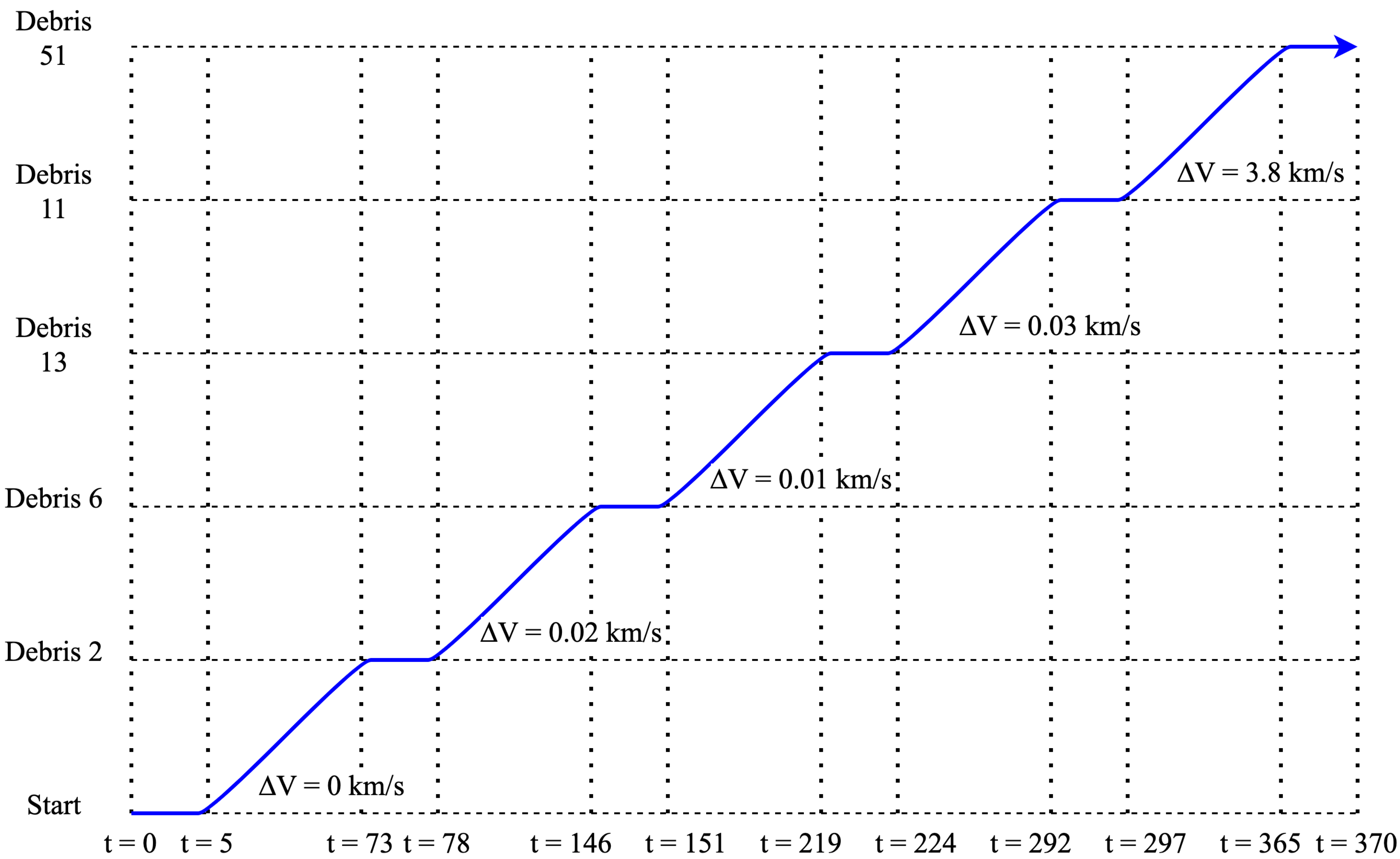

Figure C.1: Removal sequence for five removed debris

APPENDIX D

FULL RESULTS: REMOVE TEN PIECES OF DEBRIS

This appendix includes further details about the results from the case study presented in Section 4.2, including the full timeline and allocation of variables and resources over the duration of the mission.

Table D.1: Full timeline of mission to remove ten pieces of debris

Time Step	**Debris Node**	**Remaining propellant** [kg]	**ΔV** [km/s]	**Remaining Small Debris Removal Devices**	**Remaining Large Debris Removal Devices**	**Total Reward** [USD]
0	Start	20,346		10	10	0
5	Start	20,346		10	10	0
36	32	20,346		10	10	0
41	32	20,346		10	9	70,000
72	1	20,256	0.010	10	9	70,000
77	1	20,256		10	8	140,000
108	17	20,065	0.021	10	8	140,000
113	17	20,065		10	7	210,000
144	31	19,837	0.025	10	7	210,000
149	31	19,837		10	6	280,000
180	6	19,442	0.044	10	6	280,000
185	6	19,442		10	5	350,000
216	10	18,712	0.084	10	5	350,000
221	10	18,712		10	4	420,000
252	46	18,526	0.022	10	4	420,000
257	46	18,526		10	3	490,000
288	12	18,401	0.015	10	3	490,000
293	12	18,401		10	2	560,000
324	19	18,135	0.032	10	2	560,000
329	19	18,135		10	1	630,000
360	51	0	3.742	9	1	630,000
365	51	0		9	1	708,430

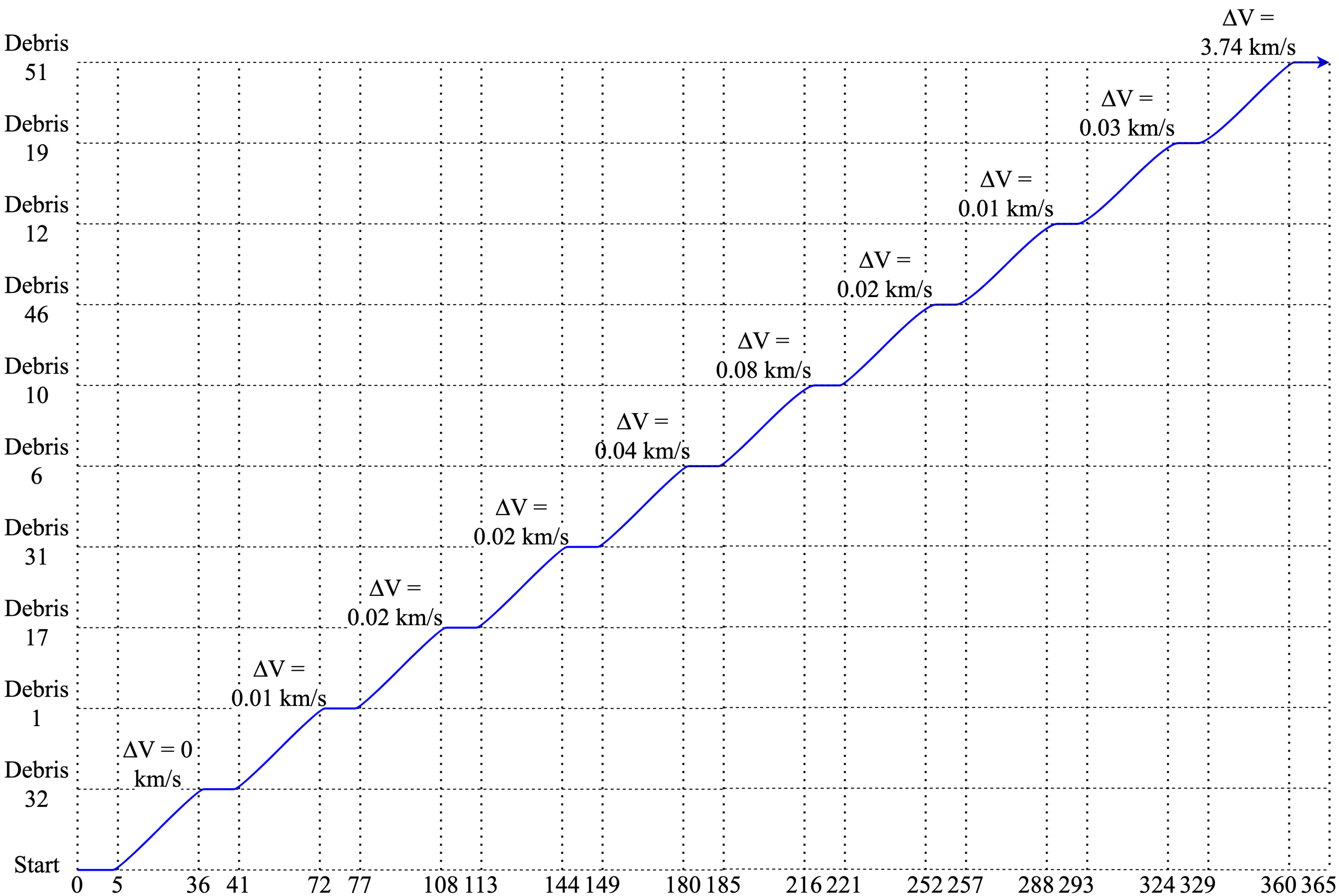

Figure D.1: Removal sequence for ten removed debris

APPENDIX E

FULL RESULTS: SUBSEQUENT LAUNCH, REMOVE FIVE PIECES OF DEBRIS

This appendix includes further details about the results from the case study presented in Section 4.3, including the full timeline and allocation of variables and resources over the duration of the mission.

Table E.1: Full timeline of subsequent mission to remove five pieces of debris

Time Step	**Debris Node**	**Remaining propellant** [kg]	**ΔV** [km/s]	**Remaining Small Debris Removal Devices**	**Remaining Large Debris Removal Devices**	**Total Reward** [USD]
0	Start	9,531		5	5	0
5	Start	9,531		5	5	0
73	31	9,531		5	5	0
78	31	9,531		5	4	70,000
146	10	9,476	0.012	5	4	70,000
151	10	9,476		5	3	140,000
219	46	9,395	0.019	5	3	140,000
224	46	9,395		5	2	210,000
292	12	9,350	0.010	5	2	210,000
297	12	9,350		5	1	280,000
365	19	9,237	0.027	5	1	280,000
370	19	9,237		5	0	350,000

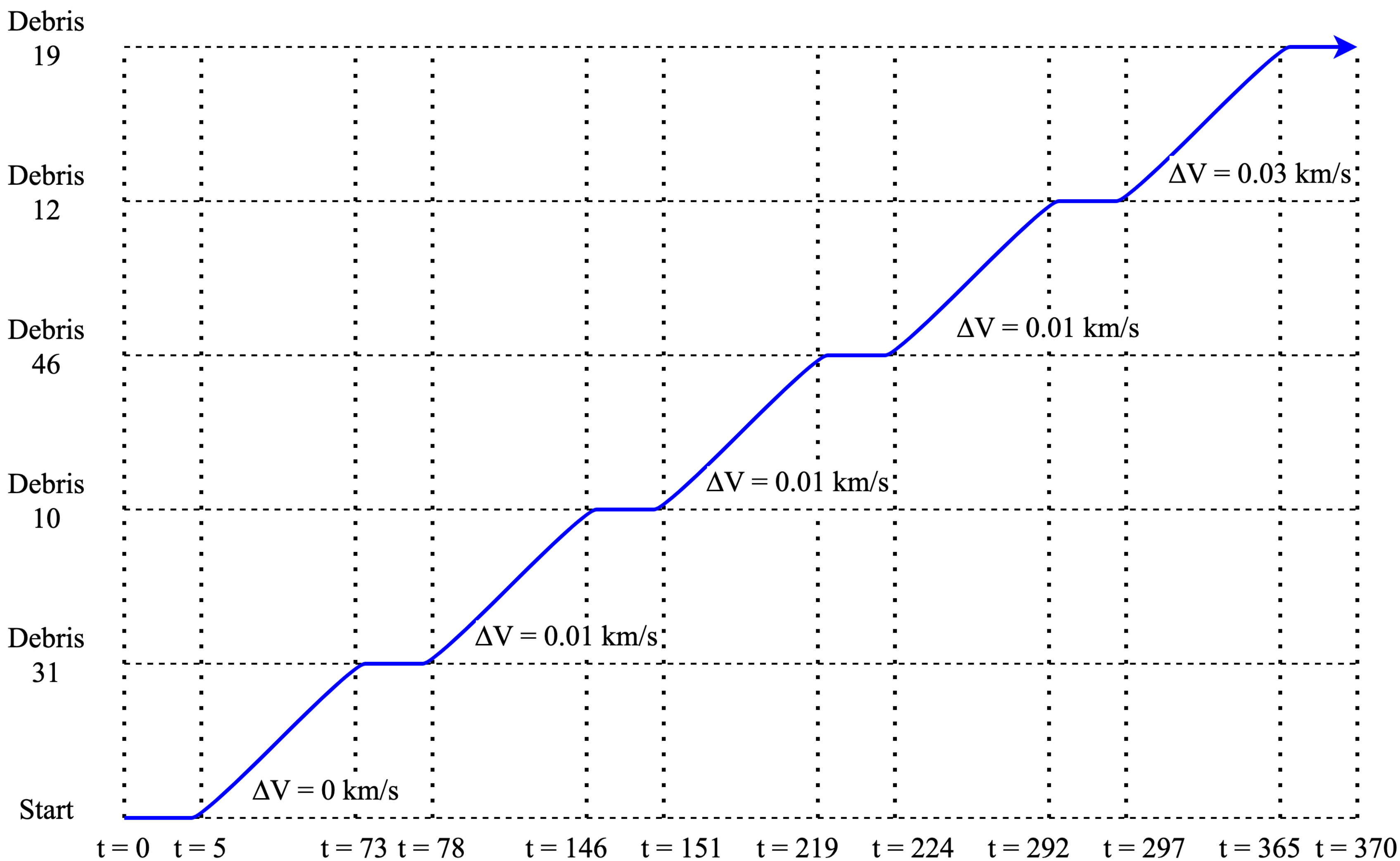

Figure E.1: Removal sequence for five removed debris in subsequent mission

APPENDIX F

FULL RESULTS: REMOVE FIFTEEN PIECES OF DEBRIS

This appendix includes further details about the results from the case study presented in Section 4.4, including the full timeline and allocation of variables and resources over the duration of the mission.

Table F.1: Full timeline of mission to remove fifteen pieces of debris

Time Step	**Debris Node**	**Remaining propellant** [kg]	**ΔV** [km/s]	**Remaining Small Debris Removal Devices**	**Remaining Large Debris Removal Devices**	**Total Reward** [USD]
0	Start	22,500		15	15	0
5	Start	22,500		15	15	0
24	5	22,500		15	15	0
29	5	22,500		15	14	70,000
48	32	22,059	0.039	15	14	70,000
53	32	22,059		15	13	140,000
72	3	21,036	0.093	15	13	140,000
77	3	21,036		15	12	210,000
96	8	20,667	0.034	15	12	210,000
101	8	20,667		15	11	280,000
120	9	20,453	0.020	15	11	280,000
125	9	20,453		15	10	350,000
144	25	19,112	0.129	15	10	350,000
149	25	19,112		15	9	420,000
168	16	18,792	0.032	15	9	420,000
173	16	18,792		15	8	490,000
192	2	18,474	0.032	15	8	490,000
197	2	18,474		15	7	560,000
216	29	17,663	0.083	15	7	560,000
221	29	17,663		15	6	630,000
240	1	16,939	0.077	15	6	630,000
245	1	16,939		15	5	700,000
264	17	16,169	0.084	15	5	700,000
269	17	16,169		15	4	770,000
288	33	15,315	0.096	15	4	770,000
293	33	15,315		15	3	840,000
312	18	14,159	0.136	15	3	840,000
317	18	14,159		15	2	910,000
336	31	14,008	0.018	15	2	910,000
341	31	14,008		15	1	980,000
360	6	13,521	0.060	15	1	980,000
365	6	13,521		15	0	1,050,000

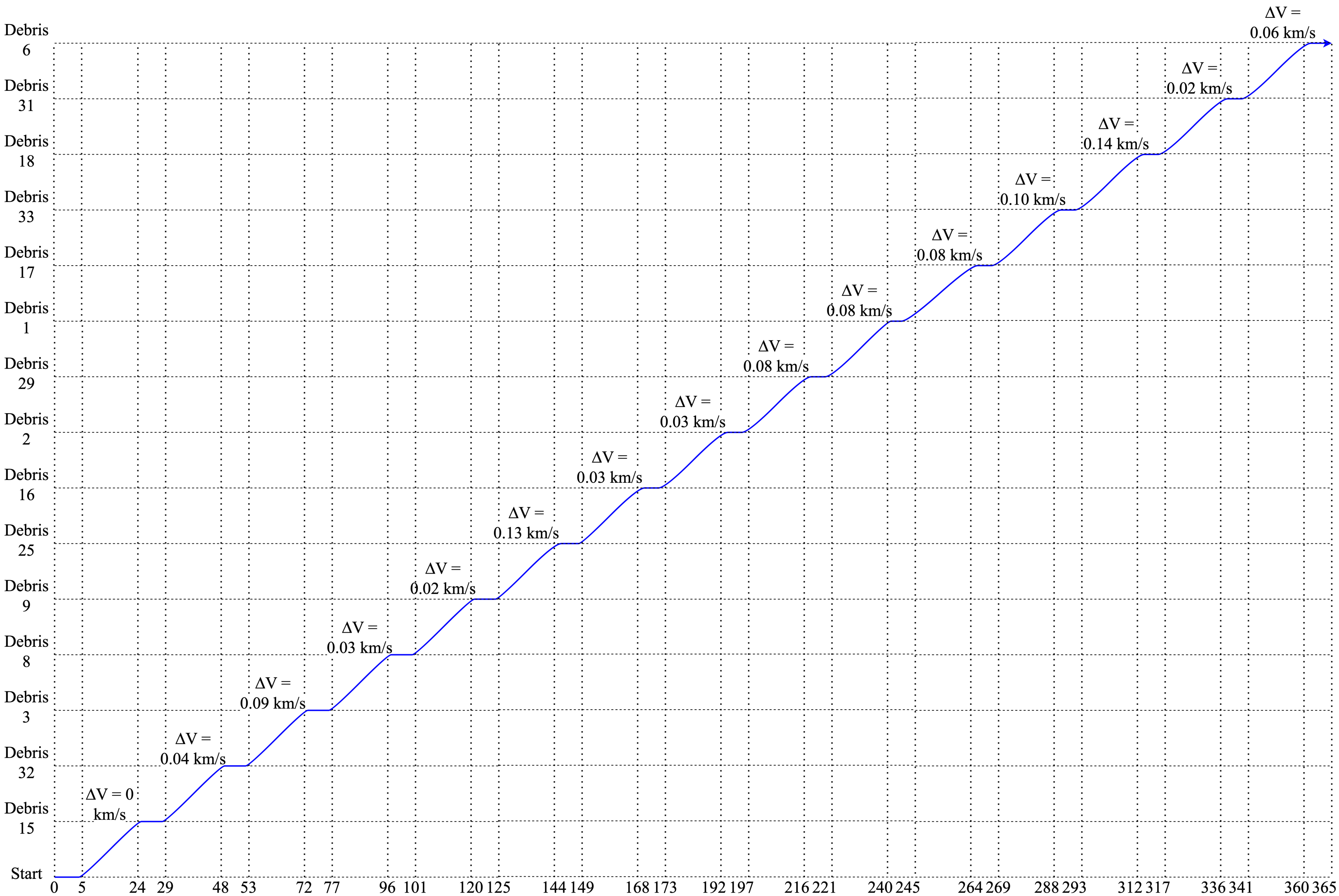

Figure F.1: Removal sequence for fifteen removed debris

APPENDIX G

PERFORMANCE STATISTICS

This appendix details the performance statistics of the optimization framework. The process to obtain an optimal solution is divided into two parts: Phase 1, which is described in Section 3.1, and Phase 2, which is described in Section 3.3. Each iteration in the binary search solves the MILP, which takes approximately 18 seconds. Phase 1 was implemented in Python using various open-source tools for astrodynamics and orbital propagation. Phase 2 was implemented in Python, and solved with GUROBI version 9.5.

The presented performance statistics were obtained by solving the case study described in Section 4.1, using the same parameters outlined in Section 4.1.1. These results were obtained on a machine with an Intel Core i7 CPU processor and 32 GB RAM under the Windows 11 operating system.

Table G.1: Optimization framework performance statistics

	Phase 1	**Phase 2**	**Total**
Time [s]	11,384	319	11703
Percentage	97.3%	2.7%	100%

REFERENCES

[1] A. Murtaza, S. J. H. Pirzada, T. Xu, and L. Jianwei, "Orbital Debris Threat for Space Sustainability and Way Forward (Review Article)," *IEEE Access*, vol. 8, pp. 61 000–61 019, 2020.

[2] D. J. Kessler and B. G. Cour-Palais, "Collision frequency of artificial satellites: The creation of a debris belt," *Journal of Geophysical Research*, vol. 83, no. A6, p. 2637, 1978.

[3] T. Wang, "Analysis of Debris from the Collision of the Cosmos 2251 and the Iridium 33 Satellites," *Science Global Security*, vol. 18, pp. 87–118, 2 Jun. 2010.

[4] J. Liou and N. Johnson, *Risks in Space from Orbiting Debris*, 2006.

[5] J.-C. Liou, N. Johnson, and N. Hill, "Controlling the growth of future LEO debris populations with active debris removal," *Acta Astronautica*, vol. 66, pp. 648–653, 5-6 Mar. 2010.

[6] T. J. Colvin, J. Karcz, and G. Wusk, "Cost and Benefit Analysis of Orbital Debris Remediation," 2023.

[7] H. X. Shen, T. J. Zhang, L. Casalino, and D. Pastrone, "Optimization of active debris removal missions with multiple targets," *Journal of Spacecraft and Rockets*, vol. 55, pp. 181–189, 1 2018.

[8] J. Yu, X. Q. Chen, and L. H. Chen, "Optimal planning of LEO active debris removal based on hybrid optimal control theory," *Advances in Space Research*, vol. 55, pp. 2628–2640, 11 Jun. 2015.

[9] N. Bérend and X. Olive, "Bi-objective optimization of a multiple-target active debris removal mission," *Acta Astronautica*, vol. 122, pp. 324–335, May 2016.

[10] M. Kanazaki and Y. Yamada, *Trajectory Optimization of a Satellite for Multiple Active Space Debris Removal Based on a Method for the Traveling Serviceman Problem*, ISBN: 9781538607435.

[11] T. Zhang, H. Shen, Y. Yang, H. Li, and J. Li, "Ant colony optimization-based design of multiple-target active debris removal mission," *Transactions of the Japan Society for Aeronautical and Space Sciences*, vol. 61, pp. 201–210, 5 2018.

[12] L. Federici, A. Zavoli, and G. Colasurdo, "A Time-Dependent TSP Formulation for the Design of an Active Debris Removal Mission using Simulated Annealing," Sep. 2019.

[13] J. Missel and D. Mortari, "Path optimization for space sweeper with Sling-Sat: A method of active space debris removal," *Advances in Space Research*, vol. 52, pp. 1339–1348, 7 2013.

[14] L. Federici, A. Zavoli, and G. Colasurdo, "On the use of A* search for active debris removal mission planning," *Journal of Space Safety Engineering*, vol. 8, pp. 245–255, 3 Sep. 2021.

[15] D. Lee, J. Lee, and J. Ahn, "Optimal Multi-target Rendezvous by Using Multi-layer Elementary Solutions," American Institute of Aeronautics and Astronautics Inc, AIAA, 2022, ISBN: 9781624106316.

[16] J. Bang and J. Ahn, "Two-phase framework for near-optimal multi-target Lambert rendezvous," *Advances in Space Research*, vol. 61, pp. 1273–1285, 5 2018.

[17] J. Bang and J. Ahn, "Multitarget rendezvous for active debris removal using multiple spacecraft," *Journal of Spacecraft and Rockets*, vol. 56, pp. 1237–1247, 4 2019.

[18] T. S. du Jonchay, H. Chen, O. Gunasekara, and K. Ho, "Framework for modeling and optimization of on-orbit servicing operations under demand uncertainties," *Journal of Spacecraft and Rockets*, vol. 58, pp. 1157–1173, 4 2021.

[19] J. C. Liou and N. L. Johnson, "A sensitivity study of the effectiveness of active debris removal in LEO," *Acta Astronautica*, vol. 64, pp. 236–243, 2-3 Jan. 2009.

[20] D. McKnight *et al.*, "Identifying the 50 statistically-most-concerning derelict objects in LEO," *Acta Astronautica*, vol. 181, pp. 282–291, Apr. 2021.

[21] N. Takeichi and N. Tachibana, "A tethered plate satellite as a sweeper of small space debris," *Acta Astronautica*, vol. 189, pp. 429–436, Dec. 2021.

[22] M. Schmitz, S. Fasoulas, and J. Utzmann, "Performance model for space-based laser debris sweepers," *Acta Astronautica*, vol. 115, pp. 376–383, Jun. 2015.

[23] V. V. Adushkin, O. Y. Aksenov, S. S. Veniaminov, S. I. Kozlov, and V. V. Tyurenkova, "The small orbital debris population and its impact on space activities and ecological safety," *Acta Astronautica*, vol. 176, pp. 591–597, Nov. 2020.

[24] D. A. Vallado and P. Crawford, "SGP4 Orbit Determination," 2014.

[25] ESA, *Pykep*, 2019.

[26] D. Izzo, "Revisiting Lambert's problem," *Celestial Mechanics and Dynamical Astronomy*, vol. 121, pp. 1–15, 1 Jan. 2015.

[27] Astroscale, "ELSA-d Press Kit," 2021.

[28] Georgia Tech Research Institute, "Guided Capture and Deorbit of Space Debris," 2022.

[29] J. E. Prussing and B. A. Conway, *Orbital Mechanics*. Oxford University Press, 1993, pp. 81–92.